

Stabilization and Activation: New Alkyl Complexes of Zinc, Magnesium and Cationic Aluminium Featuring Chelating Bisguanidine Ligands

Matthias Reinmuth,^[a] Ute Wild,^[a] Daniel Rudolf,^[a] Elisabeth Kaifer,^[a] Markus Enders,^[a] Hubert Wadepohl,^[a] and Hans-Jörg Himmel*^[a]

Keywords: Zinc / Magnesium / Aluminum / Alkyl complexes / Guanidine

In this work we report on the synthesis of new zinc, magnesium and cationic aluminium alkyl as well as Mg aryl complexes featuring chelating bisguanidine ligands [2,8-bis-(tetramethylguanidino)naphthalene (btmgn) and 1,2-bis-(tetramethylguanidino)benzene (btmgb)]. The bond properties in the complexes are analyzed with a combination of experiments and quantum chemical calculations. VT NMR

studies shed light on the fluxional processes within the complexes and their activation barriers. The compounds are stable against alkylation of the C=N imine bonds of the guanidino groups and might represent interesting alkyl transfer reagents and (co-)catalysts.

(© Wiley-VCH Verlag GmbH & Co. KGaA, 69451 Weinheim, Germany, 2009)

Introduction

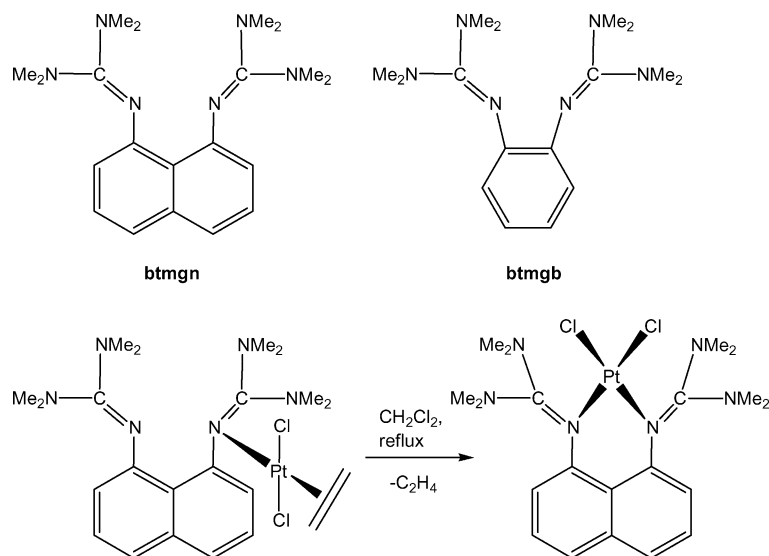
Alkyl and aryl compounds of the elements zinc, magnesium and aluminium are of interest for several applications. Hence they are widely used as alkylation agents. In addition, some of these Lewis-acidic compounds, especially with (coordinatively unsaturated) cationic Al atoms, have been shown to be alternatives to transition-metal catalysts, for example, olefin or cyclic ether polymerization.^[1,2] $[(C_5R_5)_2Al]^+$, being isoelectronic to magnesocene derivatives, $[(C_5R_5)_2Mg]$, was first synthesized by Schnöckel et al.,^[3] and later studies showed that $[(C_5H_5)_2Al]^+ [MeB(C_6F_5)_3]^-$ is an initiator for the cationic polymerization of isobutylene and the synthesis of butyl rubber.^[4] Some alkylaluminium species $[R_2Al]^+$ (R = Me, *t*Bu) were generated in toluene solutions, but turned out to be very reactive, abstracting, for example, $C_6F_5^-$ from the $[B(C_6F_5)_4]^-$ anion to form neutral aluminium and boron compounds.^[5] The isolation of the salt $[Et_2Al]^+[CB_{11}H_6X_6]^-$ (X = Cl, Br) showed that these species are indeed accessible by use of more robust anions, although even in these compounds relatively short Al...X contacts were observed.^[6] More recently, it was shown that cationic species of this sort can be stabilized by sterically shielding, bulky aryl groups. Hence in $[(2,6-Mes_2C_6H_3)_2Al]^+[B(C_6F_5)_4]^-$ the anion does not interact significantly with the almost linear, quasi-two-coordinate, diorganoaluminium cation.^[7] Generally, however, the aluminium alkyl cation is stabilized by the coordination of

additional ligands. Cationic aluminium alkyl complexes incorporating amidinate ligands were shown to polymerize ethylene under mild conditions.^[8] Olefin polymerization with such complexes was analyzed also by means of quantum chemical calculations.^[9] In the following years, a number of complexes featuring other ligands, for example, aminotroponimate,^[10] bidentate aminophenolate,^[11] imino-amide and imino-phenoxido,^[12] were synthesized and their catalytic activities evaluated. Zinc and magnesium alkyl complexes were also shown to be active in polymerization reactions.^[13]

In this work we report on the use of chelating bisguanidines as ligands in zinc, magnesium and cationic aluminium alkyl (and Mg aryl) complexes. Because of their high basicity,^[14] guanidines are interesting complex ligands. Hitherto a number of chelating bisguanidine complexes have already been prepared and characterized.^[15] Guanidine-stabilized zinc complexes were shown to be promising catalysts for the synthesis of polylactide.^[16] We reported on the synthesis of the first B(II) cationic complexes in which two guanidinate units bridge two B atoms.^[17] Recently we also synthesized the first metal complexes of the bisguanidine btmgn [bis(tetramethylguanidino)naphthalene, see Scheme 1],^[18] which had previously been shown to be a kinetically active proton sponge.^[19] The molecular structure of protonated btmgn features the proton in a bridging position between the two imine N atoms.^[19] $Pt_2(C_2H_4)_2Cl_4$ was shown to react with btmgn to give first $[(\kappa^1\text{-btmgn})PtCl_2(C_2H_4)]$ with κ^1 -coordination of the btmgn ligand and then, upon heating, $[(\kappa^2\text{-}N,N'\text{-btmgn})PtCl_2]$ with $\kappa^2\text{-}N,N'$ coordination.^[18] According to quantum chemical (DFT) calculations, the C_2H_4 elimination is associated with a change in energy and Gibbs free energy (at 298 K, 1013 mbar) of 45.4 and -3.2 kJ mol⁻¹, respectively. The molecular structure of $[(\kappa^2\text{-}$

[a] Anorganisch-Chemisches Institut, Ruprecht-Karls-Universität Heidelberg, Im Neuenheimer Feld 270, 69120 Heidelberg, Germany Fax: +49-6221-54-5707

E-mail: hans-jorg.himmel@aci.uni-heidelberg.de
Supporting information for this article is available on the WWW under <http://dx.doi.org/10.1002/ejic.200900591>.



Scheme 1.

N,N' -btmgm)PtCl₂] revealed some interesting details:^[18] (i) the naphthyl group abandons its planar structure, (ii) the Pt atom is located 133.1 pm above the “best plane” of the naphthyl aromatic system and (iii) because of different orientations of the guanidino groups relative to the naphthyl system the molecules are chiral in the crystalline phase.

On the basis of these results, we were interested in developing further the chemistry of this and related ligands by synthesizing some alkyl complexes, for example cationic aluminium complexes of the general formula [R₂Al(btmgn)]⁺ (R = alkyl). Because of the expected unusual bonding situation in these complexes it might be possible to switch relatively easily from κ^2 - to κ^1 -coordination of the btmgm ligand. This would make the complexes attractive for catalytic applications. Herein we report on the synthesis and structural characterization of the neutral alkyl complexes [Et₂Zn(κ^2 - N,N' -btmgb)], [Et₂Zn(κ^2 - N,N' -btmgm)] and [(*n*Bu)₂Mg(κ^2 - N,N' -btmgm)], the aryl complexes [(Ph)₂Mg(κ^2 - N,N' -btmgm)] and [(Ph)₂Mg(κ^2 - N,N' -btmgb)], as well as, for comparison, the more stable halides [(κ^2 - N,N' -btmgm)ZnCl₂] and [(κ^2 - N,N' -btmgm)MgBr₂], and the cationic complex [Me₂Al(κ^2 - N,N' -btmgm)]⁺ (which is isoelectronic to [R₂Mg(κ^2 - N,N' -btmgm)]). Of course the N=C double bonds of the guanidine ligands could be alkylated so that alkyl transfer reactions might occur. However it will be shown that such an alkyl transfer, although mildly exothermic according to quantum chemical calculations, does not take place.

Results and Discussion

In the following, we report on the results obtained with Zn, Mg and Al complexes. As ligands we applied 2,8-bis(tetramethylguanidino)naphthalene (btmgm, see Scheme 1)^[19] and 1,2-bis(tetramethylguanidino)benzene (btmgb, see Scheme 1).^[20]

Zn Complexes

The ethyl complex [Et₂Zn(κ^2 - N,N' -btmgb)], **1**, was prepared by a reaction between Et₂Zn and the btmgb ligand. The purity was confirmed by elemental analysis (see Exp. Sect.). A singlet signal at $\delta = 2.76$ ppm in the ¹H NMR spectrum recorded at 23 °C can be assigned to the 24 hydrogen atoms of the eight guanidino methyl groups. The CH₂ and CH₃ groups of the ethyl ligands give rise to a quartet at $\delta = -0.39$ ppm and a triplet at $\delta = 0.96$ ppm. Furthermore, two signals at $\delta = 6.75$ and 6.42 ppm belong to the aromatic ring hydrogen atoms. The IR spectrum of **1** (KBr disc) shows a very strong absorption at 1528 cm⁻¹, which can be assigned to a mode with high character from the stretch $\nu(\text{C}=\text{N})$. The corresponding band in free btmgb is located at about 1600 cm⁻¹. The large redshift upon coordination indicates a relatively strong ligand–metal interaction. Colourless crystals of **1** were grown at -21 °C by layering the toluene/THF reaction mixture with *n*-hexane. The structure as derived from X-ray diffraction is depicted in Figure 1 (see Table S1 of the Supporting Information for selected structural parameters). Interestingly, the Zn atom is located 85.1 pm above the plane defined by the aromatic C₆ ring of the ligand. While such a coordination seems to be common for the btmgm ligand (see below), it is unusual for btmgb.^[20] As expected, the ligand N=C bonds [measuring 131.8(2) and 131.6(2) pm] are slightly elongated with respect to the values in the free btmgb ligand [129.1(3) and 130.1(3) pm]. However, the imine bond lengths are still significantly smaller than, for example, in [(κ^2 - N,N' -btmgb)-PtCl₂], where 136.0(8) and 135.2(8) pm were measured.^[20] The Zn–N bond lengths amount to 223.5(1) and 222.3(1) pm and compare with distances of 222.0(5) pm in [Et₂Zn(2,2'-bipy)]^[21] and 229.4(5) pm in [Et₂Zn(tmada)].^[22] The Zn–C distances of 202.5(2) and 201.8(2) pm are also in the region typical for this class of compounds. For example, in [Et₂Zn(2,2'-bipy)], Zn–C distances of 202.2(7) pm were

found, while in $[\text{Et}_2\text{Zn}(\kappa^2\text{-}N,N'\text{-tmeda})]$ the Zn–C distances are, at 217(2) pm, slightly larger. The N1–Zn–N4 angle measures 75.02(5)°, while the C17–Zn–C19 bond angle is remarkably large (136.73°). This first result shows that bisguanidines are suitable ligands for Zn alkyls.

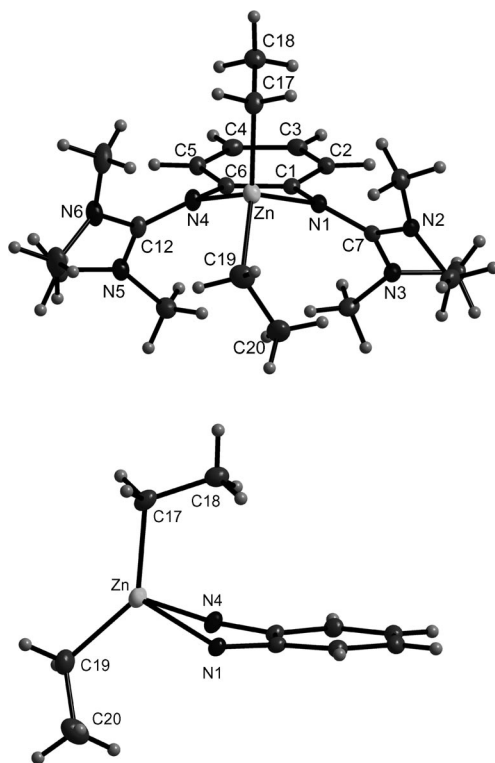


Figure 1. Molecular structure of **1**. Thermal ellipsoids drawn at the 50% probability level.

Reaction between Et_2Zn and btmgm afforded the neutral alkyl complex $[\text{Et}_2\text{Zn}(\kappa^2\text{-}N,N'\text{-btmgm})]$, **2**, which is much more air- and water-sensitive than free Et_2Zn . Coordination to the btmgm ligand seems to activate Et_2Zn significantly. The different ring size in **2** and **1** (six- vs. five-membered ring) is probably responsible for the reactivity differences. In the ^1H NMR spectrum of **2** in benzene, the protons of the ethyl groups attached to Zn give rise to a triplet at $\delta = 1.49$ ppm and a quartet at $\delta = 0.32$ ppm, shifted slightly with respect to Et_2Zn [1.09 (triplet) and 0.10 ppm (quartet) in toluene]. The guanidino CH_3 groups give rise to a strong singlet at $\delta = 2.49$ ppm. This singlet splits into four signals at lower temperature (see the VT NMR spectra shown in the Supporting Information). The fluxional processes behind these temperature effects will be discussed in detail below for the simpler case of the corresponding dichloro complex. A strong band at 1541 cm^{-1} due to the stretching modes $\nu(\text{N}=\text{C})$ in the IR spectrum argues for the presence of intact bisguanidino ligand units. Pale yellow crystals of **2** were grown directly from the reaction mixture. The molecular structure in the crystalline phase as derived from an X-ray diffraction analysis is depicted in Figure 2. Selected structural parameters are given in Table S2 (see Supporting Information). As anticipated, the btmgm ligand is bound by both imine N atoms to the Zn atom. The two guanidino

groups point to the same side of the naphthyl ring plane, in contrast to the situation in $[(\kappa^2\text{-}N,N'\text{-btmgm})\text{PdCl}_2]$ or $[(\kappa^2\text{-}N,N'\text{-btmgm})\text{PtCl}_2]$ with planar coordination at the metal.^[18] Also in contrast to these two complexes, the naphthyl system remains planar. An interesting and important detail, which will be the subject of more detailed analysis in the course of the discussion, is the position of the Zn atom 109.8 pm above the ligands' aromatic ring plane (see Figure 2). As shown here and previously (for Pd and Pt complexes^[18]), this displacement is a common feature in the coordination chemistry of the btmgm ligand. The Zn–C bond lengths of 202.0(2) and 202.0(2) pm are in good agreement with the distances measured in other complexes. However, at 218.4(2) and 214.9(2) pm the Zn–N bond lengths in **2** are significantly shorter than those in $[\text{Et}_2\text{Zn}(2,2'\text{-bipy})]$ [222.0(5) pm]^[21] or $[\text{Et}_2\text{Zn}(\text{tmeda})]$ [229.4(5) pm].^[22] They also are shorter than in **1**, arguing for stronger ligand–metal bonding. Bond lengths of 132.1(3) and 132.3(3) pm were derived for the N=C imine bonds in the guanidino groups (N4–C16 and N1–C11). For comparison, in free btmgm values of 128.1(3) and 128.3(3) pm were measured.^[19] In other complexes this bond was already shown to be elongated significantly upon complexation (cf. 135.2(7)/132.4(7) pm in $[(\kappa^2\text{-}N,N'\text{-btmgm})\text{PdCl}_2]$ and 135.7(5)/133.5(5) pm in $[(\kappa^2\text{-}$

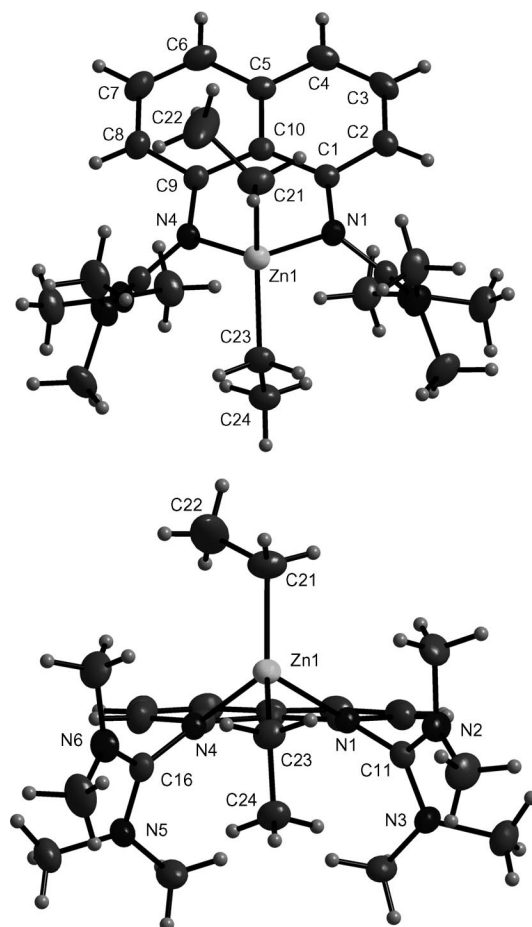


Figure 2. Molecular structure of **2**. Thermal ellipsoids drawn at the 50% probability level.

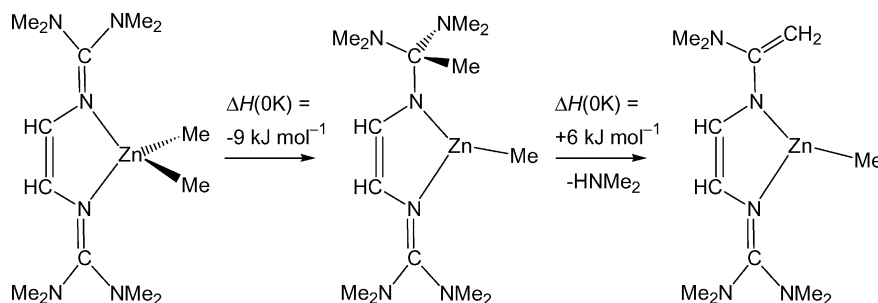
N,N'-btmgn)PtCl₂].^[18] As anticipated, the other C–N bond lengths within the guanidino groups are shorter in **2** than in free btmgn.

Complexes with dialkylzinc coordinated to 1,4-diaza-1,3-butadienes (DAB) are examples of zinc alkyls featuring chelating imine groups synthesized previously.^[23] These complexes undergo interesting reactions. Hence a complex reaction sequence is initiated by thermal- or photo-induced Zn–C bond cleavage and formation of a radical pair, one of the final products being the *N*-alkylated species. Complex **2** also features two C=N double bonds, which can be alkylated. To see if similar reactions are possible for **2**, we first carried out some quantum chemical calculations. In these calculations we used the model bisguanidine complex [Me₂Zn{C₂H₂[NC(NMe₂)₂]₂}] in which the aromatic unit is replaced by a C₂H₂ bridge (see Scheme 2 and Supporting Information). The results of these calculations indeed suggest the complex is slightly metastable with respect to alkyl transfer from Zn to the bisguanidine ligand. Transfer to the central C atom of one of the guanidino groups leads to an imine-stabilized alkylzinc amide. A gas-phase ΔH (0 K) value of -9 kJ mol^{-1} was calculated for this isomerization in the case of our model compound. This species could in a second step eliminate dimethylamine (see Scheme 2). To test this possibility experimentally, a THF solution of **2** was heated up to 80 °C in an NMR experiment. The appearance of a precipitate in this experiment argues for slow decomposition. The NMR spectra found, however, no direct evidence for alkyl transfer, which possibly points to significant barriers for such reactions. One factor at work might be steric shielding of the imino C atoms. Photolysis using broad-band irradiation emitted from a Hg high-pressure lamp resulted in no reaction. Next we tested the reactivity of **2** towards O₂. Reaction of [Me₂Zn(*t*Bu-DAB)] with O₂ was recently shown to lead to a methyl peroxide cluster.^[24] Moreover, Et₂Zn was shown to initiate radical addition of ethers such as THF to imines in the presence of air O₂.^[25] Reaction of O₂ with **2** in THF occurred very rapidly. However, a complex mixture of different products was formed, from which it proved impossible to isolate or identify a single compound.

We also synthesized, for comparison, the more stable complex [(κ^2 -*N,N'*-btmgn)ZnCl₂], **3**, which can be obtained (in contrast to **2**) very purely as shown by elemental analy-

sis. The likely structure of this molecule was previously accessed in quantum chemical calculations.^[26] Figure 3 (a) displays the structure of **3** as derived from X-ray diffraction experiments. The orientation of the two guanidino groups resembles that in **2**. The Zn–N distances are, at 201.0(2) and 200.8(2) pm, significantly shorter than in **2**. The C=N bond lengths within the guanidino groups (N1–C11 and N4–C16) measure 133.7(3) and 132.7(3) pm (see Table S3), respectively, and are thus slightly larger than in **2**. Consequently all other C–N bonds involving the C atoms C11 and C16 are shorter. This implies that the degree of electron donation from the btmgn ligand to the ZnCl₂ unit is slightly stronger than to Et₂Zn, in line with the higher electronegativity of the Cl atoms.

To obtain more information about the conformational properties, we carried out variable temperature (VT) ¹H NMR studies for **3** in CH₂Cl₂ solutions. Similar studies had already been performed for the free bisguanidine btmgn before and after protonation^[19] as well as for the complexes [(κ^2 -*N,N'*-btmgn)PdCl₂] and [(κ^2 -*N,N'*-btmgn)PtCl₂].^[27] In the case of [(κ^2 -*N,N'*-btmgn)PdCl₂], three different fluxional processes of the guanidino groups were identified and their rate constants determined. Figure 3 (b) shows the measured VT ¹H NMR spectra of **3** in CH₂Cl₂ together with spectra from the results of line shape analysis (see also the spectra in the Supporting Information for **3** dissolved in CD₃CN in the temperature range -30 °C to $+60 \text{ °C}$). In contrast to [(κ^2 -*N,N'*-btmgn)PdCl₂], for which the ¹H NMR spectrum at 178 K showed eight signals (the maximum number), the CH₃ groups in **3** split into four signals at this temperature. The ¹H signals at the aromatic ligand backbone give only three multiplets. Together with the observation of four CH₃ signals, this shows that the two tetramethylguanidino moieties are equivalent. The four CH₃ NMR signals have been assigned to the CH₃ groups as depicted in Scheme 3. The assignment was made on the basis of NOE correlations. The fluxional processes in **3** with the metal coordinated in a distorted tetrahedral fashion are thus significantly different to those found in the Pd^{II} and Pt^{II} complexes where the metal is coordinated in a distorted square-planar fashion. The analysis of the spectra gave evidence for two dynamical processes. At low temperature the interchange between the methyl groups 1 and 4 as well as 2 and 3 (see Scheme 3, with a rate constant k_1) becomes



Scheme 2.

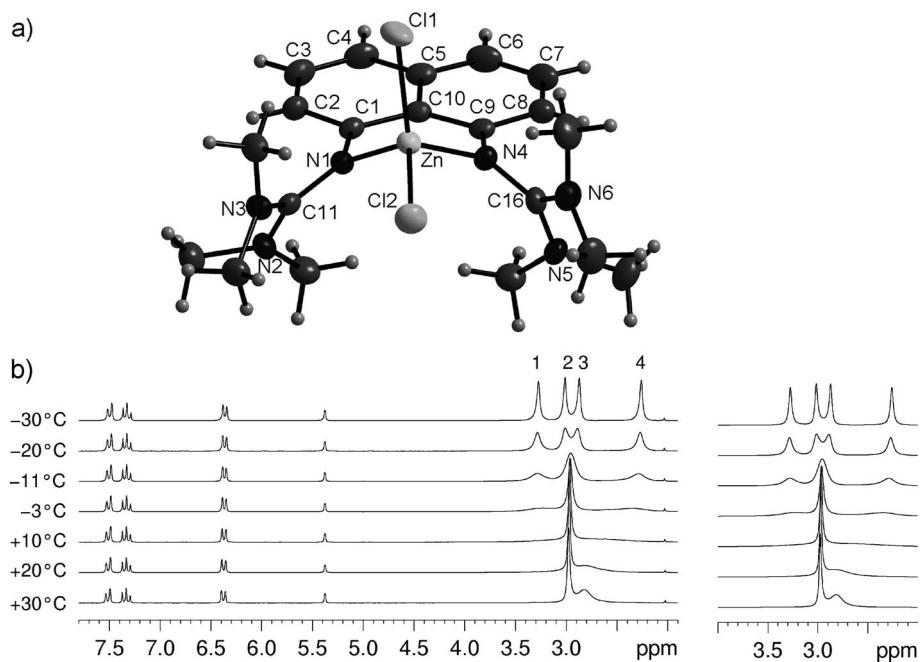
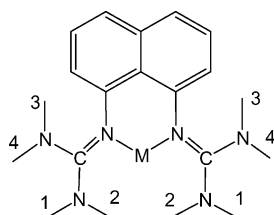


Figure 3. (a) Molecular structure of **3**. Thermal ellipsoids drawn at the 50% probability level. (b) VT NMR spectra of **3** in CH_2Cl_2 (left side), together with the results of line shape analysis simulations (right side). The numbers (1–4) correspond to the CH_3 positions shown in Scheme 3.

observable. This process can also be described as a motion of the Zn atom from one side of the aromatic plane to the other. Arrhenius and Eyring plots derived from the temperature dependence of the rate constants yielded estimates for the activation enthalpy and entropy. At standard conditions, ΔH^\ddagger amounts to $(+43 \pm 2) \text{ kJ mol}^{-1}$ and $\Delta S^\ddagger = (-41 \pm 10) \text{ J mol}^{-1}$. A second process can be described as rotation around the C–N bonds (with a rate constant k_2), leading to interchange of the methyl groups 3 and 4 as well as 1 and 2 (see Scheme 3). In this case a standard activation enthalpy of $(+45 \pm 2) \text{ kJ mol}^{-1}$ [$\Delta S^\ddagger = (-67 \pm 10) \text{ J mol}^{-1}$] was obtained.



Scheme 3.

Mg Alkyl and Aryl Complexes

The Mg alkyl complex $[(n\text{Bu})_2\text{Mg}(\kappa^2\text{-}N,N'\text{-btmgn})]$, **4**, was synthesized by a reaction between $(n\text{Bu})_2\text{Mg}$ (1 M in *n*-heptane) and btmgn dissolved in toluene. It turned out to be an extremely unstable compound, so that we were not able to characterize it adequately. In the ^1H NMR spectrum of **4** in toluene, a number of broad signals in the region from 2.09 to -0.45 ppm can be assigned to the two *n*-butyl

groups. The guanidino methyl groups give rise to a broad signal around 2.40 ppm. This singlet splits again into four signals at low temperatures. Pale yellow crystals were obtained by layering the solution with *n*-hexane at -20 °C. The molecular structure as derived from X-ray diffraction is shown in Figure 4. Selected structural parameters can be found in Table S4 (see Supporting Information). The quality of the structure determination is hampered by the presence of highly disordered solvent molecules (alkanes from petroleum ether) in the crystal and by additional disorder of the *n*-butyl substituents (see Experimental Section). Interesting details of the molecular structure include: (i) the position of the Mg atom being 121.3(2) pm displaced from the plane of the btmgn ligand and (ii) the short N=C bond lengths of 132.2(5) and 132.4(4) pm, indicating the weak donor character of the btmgn ligand and consequently rela-

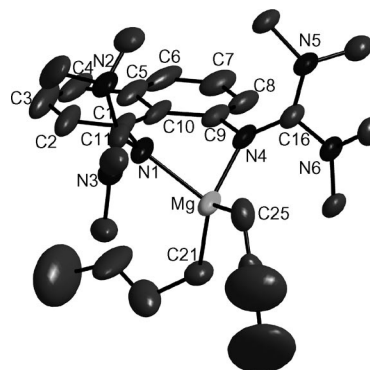
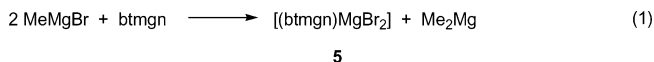


Figure 4. Molecular structure of **4**. Thermal ellipsoids drawn at the 50% probability level.

tively weak ligand–metal bonding. Quantum chemical calculations again suggest the isomer formed by alkyl transfer from the Mg atom to the imine C atom is more stable [ΔH (0 K) = -15 kJ mol^{-1}]. However, similar to the situation in the Zn compounds, no direct evidence for alkyl transfer was observed. Nevertheless, the compound is highly unstable and decomposes already at room temperature. We also synthesized the related alkyl complex [$\text{Me}_2\text{Mg}(\kappa^2\text{-N,N}'\text{-btmgn})$], but this complex turned out to be even more sensitive.

As in the case of the Zn alkyl complexes, we synthesized for comparison a more stable Mg halide complex, with the main aim of analyzing the fluxional processes and to compare the results with the Zn complex. Especially the evaluation of the vibration of the metal atom from one side of the ligands' aromatic ring plane to the other should provide useful information about the bond properties. However, it turned out to be surprisingly difficult to synthesize such a compound with the required purity. Probably the best access turned out to be a reaction between a Grignard com-

pound such as MeMgBr and the ligand btmgn . The complex [$\kappa^2\text{-N,N}'\text{-btmgn})\text{MgBr}_2$], **5**, is formed according to Equation (1) (neglecting any Schlenk equilibrium).



Crystals of **5** were obtained and the molecular structure determined by X-ray diffraction. The compound crystallizes together with equimolar amounts of THF. The resulting molecular structure is displayed in Figure 5a. Table S5 (see Supporting Information) lists some structural parameters. The shorter Mg–N bond lengths [204.9(3)/205.2(3) pm in **5** vs. 214.0(3)/215.2(3) pm in **4**] signal stronger ligand–metal bonding in **5** than in **4**. The Mg atom is located 116.6 pm above the btmgn aromatic plane. Figure 5 (b) shows the VT ^1H NMR spectra experimentally measured and simulated. At r.t., only one signal of the CH_3 groups is observed ($\delta = 3 \text{ ppm}$), which splits into four signals at lower temperatures. Two additional signals at $\delta = 1.89$ and 4.00 ppm can be assigned to THF, which was cocrystallized with the guan-

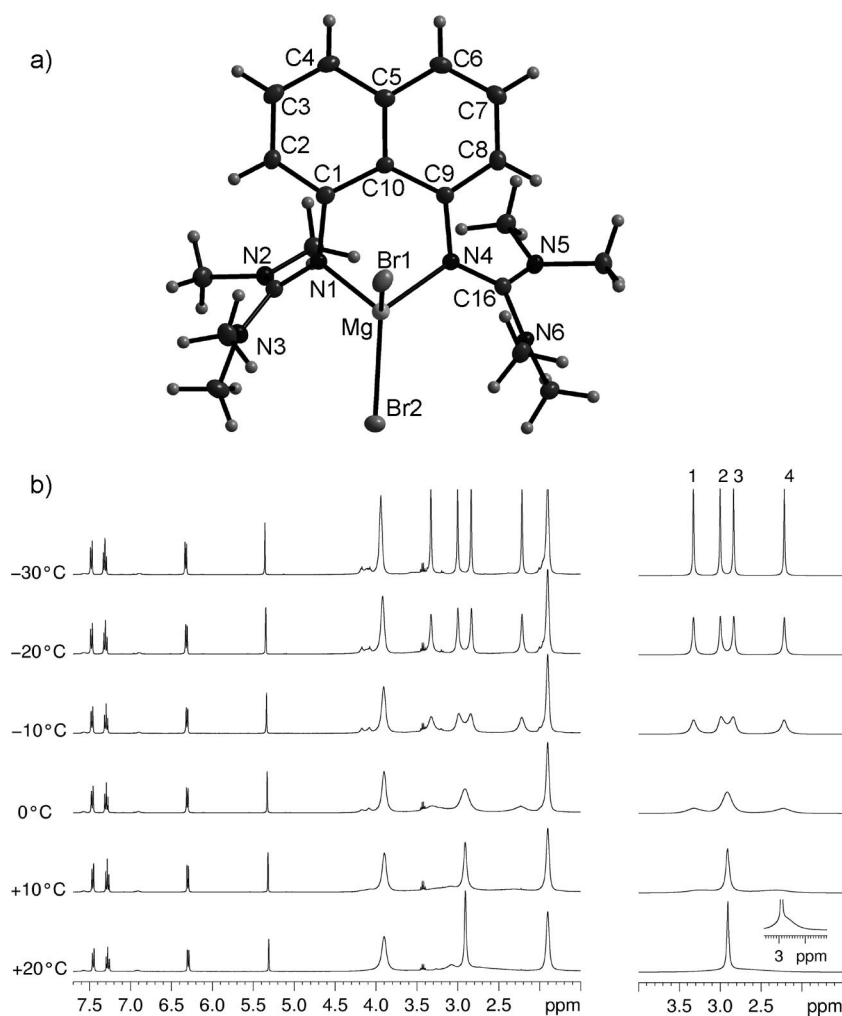


Figure 5. (a) Molecular structure of **5**. Thermal ellipsoids drawn at the 50% probability level. (b) VT NMR spectra of **5** in CH_2Cl_2 (left side), together with the results of line shape analysis simulations (right side). The numbers (1–4) correspond to the CH_3 positions depicted in Scheme 3.

idine complex. The dynamic behaviour can be modelled with an interchange between methyl groups 2–3 and 1–4 (see Scheme 3), corresponding to a motion of the Mg atom from one side of the ligand aromatic ring to the other. The activation parameters for this process have been determined as $\Delta H^\ddagger = (53 \pm 2) \text{ kJ mol}^{-1}$ and $\Delta S^\ddagger = (-4 \pm 8) \text{ J mol}^{-1}$. The activation entropy value around zero is in accordance with a unimolecular process and low steric hindrance in the transition state. As the chemical exchanges of the CH_3 resonances are monomolecular processes, activation entropies are expected which are around zero for transition states that are not sterically encumbered or negative when more restrictions are present in the transition states. Thus, the smaller Zn (or Al, see below) ions lead to more negative activation entropies compared to complex **5** with the larger Mg ion.

As an example of a Mg aryl complex we synthesized $[\text{Ph}_2\text{Mg}(\kappa^2\text{-}N,N'\text{-btmgb})]$, **7**. This complex turned out to be significantly more stable than the alkyl complex **4**, and also complex **6**. Therefore it can be isolated more easily in relatively high yield (85%, see Exp. Sect.). Unfortunately only small crystals which appeared to be twinned were obtained, so that a satisfying X-ray diffraction analysis was impossible. Better analytical data can be obtained with the aryl complex $[\text{Ph}_2\text{Mg}(\kappa^2\text{-}N,N'\text{-btmgn})]$, **6**, which can be pre-

pared by reaction between $\text{Ph}_2\text{Mg}^{[28]}$ and btmgn. In the ^1H NMR spectrum recorded in benzene, the two phenyl groups give rise to extra signals at $\delta = 8.16$ ppm (protons in the *ortho* positions) and in the region 7.48–7.18 ppm. This time two signals due to the guanidino methyl groups (at $\delta = 2.51$ and 1.85 ppm) already appear at 303 K, arguing for differences in the fluxional processes with respect to the other Mg complexes. The two signals further split to give a quartet at low temperatures (233 K). Figure 6 displays its molecular structure (see Table S6 for structural information). Again, the two imine $\text{N}=\text{C}$ bonds of the guanidino groups point to the same side, so that the two phenyl groups experience different environments. As expected, the $\text{Mg}-\text{N}$ distances in **6** are slightly shorter than in **4** [210.6 and 212.6 pm in **6** vs. 214.0(3) and 215.2(3) pm in **4**], but longer than in **5**. With $87.5(1)^\circ$, the $\text{N}-\text{Mg}-\text{N}$ angle in **6** is larger than in **4**.

Synthesis of Stable Cationic Al Alkyl Complexes

A major aim of this work was the synthesis and characterization of a stable cationic Al alkyl complex featuring btmgn or btmgb as the ligand. We used the monoprotonated form of btmgn^[19] for the synthesis of $[\text{Me}_2\text{Al}(\kappa^2\text{-}N,N'\text{-btmgn})]^+$, **8**, according to Equation (2). A similar strategy was used previously for the preparation of other cationic aluminium alkyl species, for example, recently by Coles et al. in the case of $[\text{H}_2\text{C}\{\text{hpp}\}_2\text{AlMe}_2]^+[\text{BPh}_4]^-$ ($[\text{8}(\text{B}(\text{C}_6\text{H}_5)_4)]^-$, see Scheme 4, hpp = 1,3,4,6,7,8-hexahydro-2*H*-pyrimido[1,2-*a*]pyrimidine).^[29] We tried to crystallize the new cationic Al alkyl complex with $[\text{PF}_6]^-$, $[\text{B}(\text{C}_6\text{H}_5)_4]^-$ and $[\text{B}(\text{C}_6\text{F}_5)_4]^-$ as counterions and finally obtained crystals suitable for X-ray diffraction for the salt $[\text{8}(\text{BPh}_4)]$ (see Figure 7). This salt turned out to be stable and was obtained in good yield and purity according to elemental analysis. In the mass spectrum the most intense signal shows at $m/z = 411$ ($[\text{M}]^+$). In the ^1H NMR spectrum measured at room temp. a singlet at -0.88 ppm can be assigned to the two methyl groups attached to Al. The X-ray diffraction measurements gave a molecular structure in which the Al atom is located 79.0 pm above the plane defined by the naphthyl group. The Al–C and Al–N bond lengths were measured to be 197.0(5)/197.3(5) and 191.8(3) pm, respectively (see also Table S7 in the Supporting Information). These values are close to those obtained for the related species **9**, **10** and **11** (see Scheme 4). Thus the salt $[\text{9}(\text{BPh}_4)]$ features Al–C and Al–N bond lengths of 197.0(4)/196.4(3) and 190.7(2)/192.0(2) pm, respectively.^[29] Al–C and Al–N bond lengths of 201.0(2)/201.6(2) and 193.4(2)/193.2(2) pm, respectively, were measured in $[\text{10}(\text{B}(\text{C}_6\text{F}_5)_4)]$ (see Scheme 3).^[30] Finally, in $[\text{11}(\text{B}(\text{C}_6\text{F}_5)_4)]$ (see Scheme 4) Al–C and Al–N bond lengths of 196.4(3)/199.3(3) and 189.4(2)/193.5(2) pm, respectively, were obtained.^[31] With $109.6(2)^\circ$ the $\text{N}-\text{Al}-\text{N}$ angle is significantly larger than in all other compounds discussed in this work.

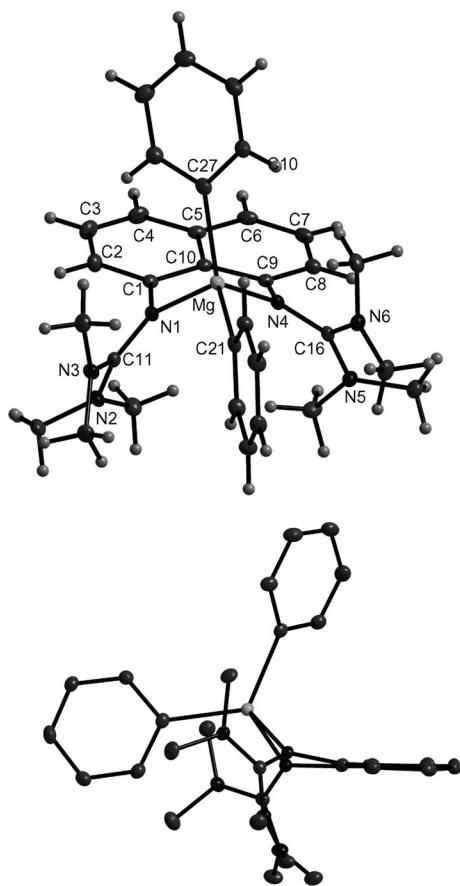
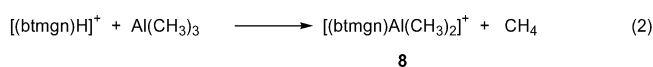
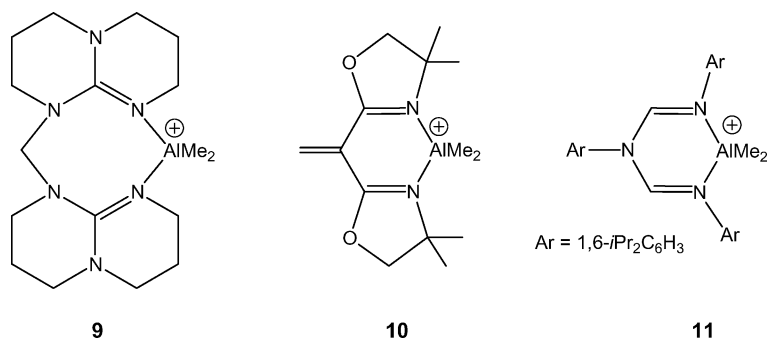


Figure 6. Molecular structure of **6**. Thermal ellipsoids drawn at the 50% probability level. The side view (hydrogen atoms omitted for sake of clarity) is also provided.





Scheme 4.

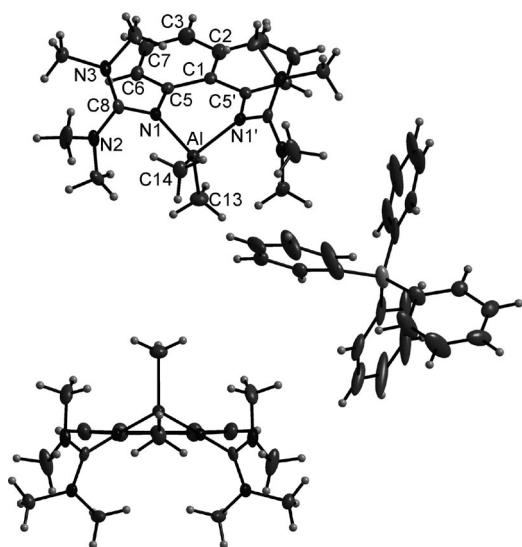


Figure 7. Molecular structure of **8**[BPh₄]. Thermal ellipsoids drawn at the 50% probability level. A side view of the molecular structure of **8** is shown underneath.

Reaction of the salt [(btmgbH)B(C₆F₅)₄], prepared from equimolar amounts of btmgb and [H(OEt)₂][B(C₆F₅)₄], with AlMe₃ yielded the cationic alkyl-Al complex [Me₂-Al(κ²-N,N'-btmgb)][B(C₆F₅)₄]. However, it was not possible to grow crystals of sufficient quality for an XRD analysis.

Quantum chemical (DFT) calculations were applied to estimate the strength of the bonding between the btmgn ligand and the Me₂Al⁺ unit in **8**. The energy required for conversion from κ²- to κ¹-coordination of the btmgn ligand (see Figure 8) amounts to 151 kJ mol⁻¹ according to BP86/SV(P). The geometry of the btmgn ligand and the location of the metal in [Me₂Al(κ¹-btmgn)]⁺ with a three-coordinate Al atom resembles that of [(κ¹-btmgn)PtCl₂(C₂H₄)] (see Scheme 1).^[18] It is possible that the Al atom of this complex can interact with an ethylene unit if the complex is used for ethylene polymerization. The complete removal of the btmgn unit requires a further 362 kJ mol⁻¹.

Finally, a VT ¹H NMR study of complex **8** was carried out (see Figure 9, only the region containing the guanidine and aluminium methyl group signals is shown). A consequence of freezing the motion of the metal from one side of the ligands' aromatic system to the other on the NMR

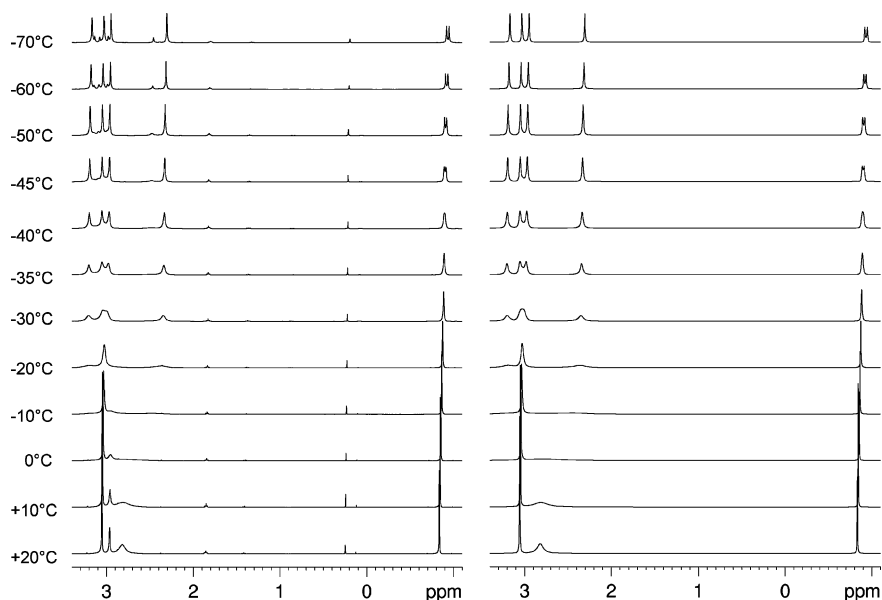


Figure 8. VT NMR spectra of **8**[PF₆] in CH₂Cl₂ (left side), together with the results of line shape analysis simulations (right side).

timescale is the nonequivalence of the two methyl groups attached to the Al atom. The observation of an Al-methyl signal splitting at low temperatures thus serves as direct confirmation of the correct description of the process. Moreover, the spectra simulation showed that the interchange between the guanidino and the aluminium methyl groups occurs with the same rate constant. From Eyring plots the activation enthalpy and entropy for this process can be estimated to be $(+41 \pm 2) \text{ kJ mol}^{-1}$ and $(-35 \pm 9) \text{ J mol}^{-1}$, respectively. The activation parameters of **8** are therefore very similar to the parameters determined for the btmgn-ZnCl_2 complex **3**.

in **9** [189.9(2) and 190.6(3) pm] are significantly shorter than those measured in **10** [197.9(5) and 198.2(6) pm]. Consequently, with 216.72(10) and 216.01(9) pm, the Ga–Cl bond lengths in **9** are larger than those in **10** [210.5(2) and 210.4(2) pm]. The metal atom in **9** is again displaced (by 74.0 pm) from the plane defined by the aromatic rings. Other structural parameters are listed in Table S8. Compound **10** exhibits a relatively low melting point of 155–156 °C. With 242 °C, the melting point of **9** is significantly higher.

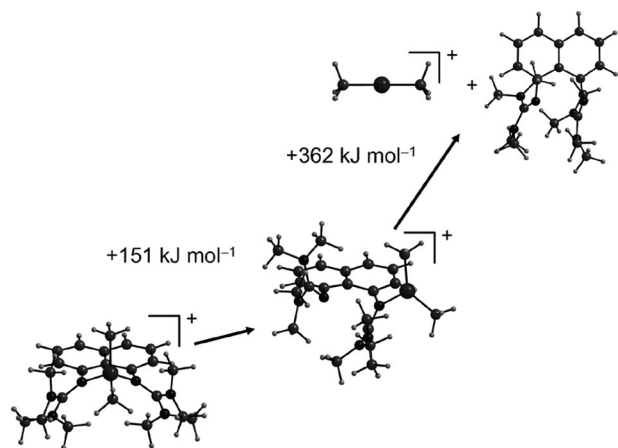


Figure 9. Quantum chemical (DFT) calculations on the change from $\kappa^2\text{-N,N}'$ to κ^1 -coordination of the btmgn ligand in **8**.

Cationic gallium halide complexes are easily accessible. Hence GaCl_3 reacts with btmgn to give the salt $[(\kappa^2\text{-N,N}'\text{-btmgn})\text{GaCl}_2]^+[\text{GaCl}_4]^-$, **9**, according to Equation (3). The first evidence for the formation of such a salt came from mass spectroscopy. Hence the mass spectra (FAB^+) displayed a strong signal at $m/z = 495.2$ because of the $[(\text{btmgn})\text{GaCl}_2]^+$ cation. The product was then confirmed by XRD analysis of single crystals grown from THF solutions. Figure 10 illustrates the molecular structure obtained from this analysis. Similar reactions were previously reported for diimines. For example, it had been shown that DAB (1,4-di-*tert*-butyl-1,4-diazabutadiene) reacts with GaCl_3 to give $[(\text{DAB})\text{GaCl}_2][\text{GaCl}_4]$ (**10**).^[32] Because of the higher basicity of the btmgn ligand, the Ga–N bond lengths

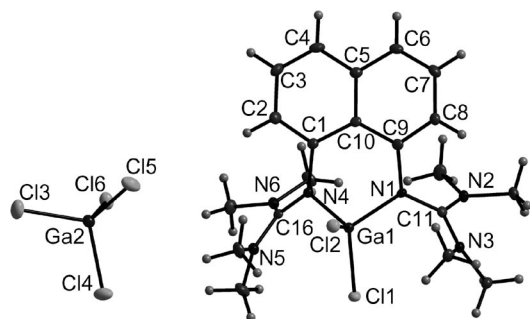


Figure 10. Molecular structure of **9**. Thermal ellipsoids drawn at the 50% probability level.

Conclusions

In this work we reported on the synthesis and characterization of the first zinc, magnesium and cationic aluminium alkyl and aryl complexes of the bisguanidino ligands btmgb and btmgn (see Scheme 1). For comparison and further analysis, we also isolated some corresponding halide complexes. Generally, the metal-organic complexes turned out to be highly reactive and sensitive. As expected, the average $\text{N}=\text{C}$ bond length in the guanidino units increases over the course of complex formation. The following order is observed for the metal complexes of btmgn known so far: btmgn (128.2 pm)^[19] < $[(n\text{Bu})_2\text{Mg}(\kappa^2\text{-N,N}'\text{-btmgn})]$ (132.0 pm) < $[\text{Et}_2\text{Zn}(\kappa^2\text{-N,N}'\text{-btmgn})]$ (132.2 pm) < $[\text{Ph}_2\text{Mg}(\kappa^2\text{-N,N}'\text{-btmgn})]$ (133.0 pm) < $[(\kappa^2\text{-N,N}'\text{-btmgn})\text{-ZnCl}_2] \approx [(\kappa^2\text{-N,N}'\text{-btmgn})\text{MgBr}_2]$ ($\delta = 133.2$ ppm) < $[(\kappa^2\text{-N,N}'\text{-btmgn})\text{PdCl}_2]$ ($\delta = 133.8$ ppm)^[18] < $[(\kappa^2\text{-N,N}'\text{-btmgn})\text{-NiCl}_2]$ ^[33] ($\delta = 134.1$ ppm) < $[(\kappa^2\text{-N,N}'\text{-btmgn})\text{PtCl}_2]$ ^[18] ($\delta = 134.6$ ppm) $\approx [\text{Me}_2\text{Al}(\kappa^2\text{-N,N}'\text{-btmgn})]^+$ (134.5 pm) < $[(\kappa^2\text{-N,N}'\text{-btmgn})\text{GaCl}_2]^+$ ($\delta = 136.0$ ppm). The electron donation from btmgn to the metal increases in the same order and the stability of the complexes follows a similar order. Hence the magnesium and zinc alkyl complexes are highly unstable and decompose slowly in solution already at room temperature, while the cationic aluminium complex is remarkably stable. Another interesting detail is the displacement of the metal atom from the plane defined by the aromatic system. This displacement reaches a maximum of 121.3 pm in $[(n\text{Bu})_2\text{Mg}(\kappa^2\text{-N,N}'\text{-btmgn})]$ and is relatively small in $[\text{Me}_2\text{Al}(\kappa^2\text{-N,N}'\text{-btmgn})]^+$ (79.0 pm). Complexes of the bisguanidino btmgb are generally more stable than the corresponding ones of btmgn. Alkylation of the $\text{C}=\text{N}$ double bonds of the guanidino groups was not observed, although intramolecular alkyl transfer is mildly exothermic according to quantum chemical calculations.

All compounds in this study showed dynamic behaviour at the CH_3 groups of the guanidino units. A detailed VT NMR analysis of compounds **3**, **5** and **8** shows that the fast exchange between two pairs of CH_3 signals is due to a movement of the metal atoms from one side of the naphthyl backbone to the other side. This movement also exchanges the positions of the additional ligands (e.g., the two Al– CH_3 groups in **8**). The rotations around the $\text{C}-\text{MCl}_2$ bonds of

the guanidino groups occur at slower rates, so that at high temperatures all four guanidine-CH₃ signals collapse into one singlet.

Ongoing studies in our group focus on *i.* direct applications of these alkyl complexes in catalysis,^[34] *ii.* the possibility to synthesize cationic alkyl complexes stabilized by the strong electron-donating character of the bisguanidino ligands and *iii.* the possibility to use the complexes as starting reagents for the preparation of di- and oligonuclear alkyl complexes.

Experimental Section

General: The bisguanidine btmgm was purchased from Fluka (grade: "purum"). Et₂Zn solutions in toluene (1.5 M) were delivered by Acros. Me₃Al (2 M in toluene) was purchased from Aldrich. While all compounds are air- and water-sensitive, there are some distinctive reactivity differences. Thus compound **2** is the most sensitive among the Zn complexes reported herein. The Mg alkyl complexes show signs of decomposition already at room temp. IR spectra were recorded with a Bruker Vertex 80v spectrometer. VT NMR measurements were performed on a Bruker DPX200 and a Bruker AvanceII 400 spectrometer equipped with an N₂ gas/liq. N₂ heat exchanger and a BVT 3200 control unit [NMR chemical shifts relative to TMS (¹³C and ¹H), BF₃·OEt₂ (¹¹B), H₃PO₄ (³¹P) and CFCl₃ (¹⁹F)]. The temperature was calibrated with a [D₄]MeOH NMR thermometer.^[35] "PE 40/60" stands for petroleum ether with a boiling range of 40–60 °C.

[Et₂Zn(κ²-N,N'-btmgb)] (1): btmgb (0.100 g, 0.329 mmol) was dissolved in THF (2 mL). After dropwise addition of an Et₂Zn solution (0.3 mL, 1.5 M) in toluene the reaction mixture was stirred for 2 h. Layering of the solution with *n*-hexane (4 mL) and storage at –21 °C yielded colourless crystals of [Et₂Zn(κ²-N,N'-btmgb)] (yield 79%). C₂₀H₃₈N₆Zn (427.93): calcd. C 56.13, H 8.95, N 19.64, Zn 15.28; found C 56.27, H 9.03, N 19.52. ¹H NMR (400 MHz, CD₂Cl₂, 23 °C): δ = 6.75 (m, 2 H, CH_{arom.}), 6.42 (m, 2 H, CH_{arom.}), 2.76 (m, 24 H, Me), 0.96 (t, 6 H, ZnCH₂CH₃), –0.39 (q, 4 H, ZnCH₂CH₃) ppm. ¹³C{¹H} NMR (100.55 MHz, CD₂Cl₂, 23 °C): δ = 143.75 (arom. C), 121.60 (arom. CH), 121.04 (arom. CH), 39.77 (NCH₃), 14.61 (CH₃), 3.49 (CH₂) ppm. IR (KBr): ν̄ = 3046 (w), 3003 (w), 2924 (m), 2866 (m), 2831 (m), 2694 (w), 1528 (vs) 1468 (s), 1390 (vs), 1338 (m), 1273 (m), 1236 (m), 1211 (m), 1148 (s), 1109 (m), 1061 (m), 1022 (s), 984 (m), 928 (m), 870 (w), 826 (m), 737 (vs), 706 (m), 627 (w), 590 (m), 560 (m) cm^{–1}.

[Et₂Zn(κ²-N,N'-btmg)] (2): btmgm (103 mg, 0.29 mmol) was dissolved in dry THF (5 mL) and an Et₂Zn solution (0.3 mL, 1.5 M) in toluene was added dropwise. The clear yellow reaction mixture was stirred for a period of 2 h at room temperature. Subsequently the solution was layered with *n*-hexane at –20 °C to obtain pale yellow crystals (73 mg, 0.15 mmol, 52% yield). C₂₄H₄₀N₆Zn (477.98): calcd. C 60.31, H 8.43, N 17.58; found C 58.31, H 8.03, N 16.13. ¹H NMR (399.89 MHz, C₆D₆, 296.2 K): δ = 7.45 (dd, *J* = 8.16, 1 Hz, 2 H, CH_{arom.}), 7.26 (t, *J* = 7.69 Hz, 2 H, CH_{arom.}), 6.32 (m, 2 H, CH_{arom.}), 2.49 (m, 24 H, CH₃), 1.49 (m, 6 H, ZnCH₂CH₃), 0.32 (m, 4 H, ZnCH₂CH₃) ppm. ¹³C NMR (100.56 MHz, C₆D₆, 297.4 K): δ = 149.90, 138.07, 125.98, 123.48, 121.45, 116.52 (C_{arom.}), 39.65 (CH₃), 15.35 (CH₃), 3.73 (CH₂) ppm. ¹H NMR (399.89 MHz, [D₈]THF, 296.2 K): δ = 7.20 (d, *J* = 7.91 Hz, 2 H), 7.09 (t, *J* = 7.68 Hz, 2 H), 6.15 (d, *J* = 7.30 Hz, 2 H), 2.75 (m, 24 H, CH₃), 0.92 (m, 6 H, CH₃), –0.33 (m, 4 H, CH₂

ppm. ¹³C NMR (100.56 MHz, [D₈]THF, 297.4 K): δ = 150.46, 138.59, 126.20, 123.93, 121.55, 116.91 (C_{arom.}), 40.27 (CH₃), 14.45 (CH₃), 3.55 (CH₂) ppm. ¹H NMR (200 MHz, [D₈]THF, 203 K): δ = 3.16 (s, 4 H), 2.95 (s, 4 H), 2.79 (m, 8 H), 2.60 (s, 4 H), 2.15 (s, 4 H) ppm. IR (KBr): ν̄ = 3043 (w), 3002 (w), 2929 (s), 2861 (s), 2787 (sh), 1541 (vs), 1462 (vs), 1398 (vs), 1372 (vs), 1279 (m), 1234 (s), 1145 (s), 1061 (s), 988 (s), 925 (m), 837 (s), 761 (s), 686 (m), 584 (m), 472 (m) cm^{–1}.

[(κ²-N,N'-btmg)ZnCl₂] (3): btmgm (216.8 mg, 0.61 mmol) was dissolved in CH₃CN (12 mL) and a ZnCl₂ solution (0.6 mL, 1 M) in Et₂O was added dropwise. The reaction mixture was stirred for 24 h at room temperature. Subsequently the solvent was removed under vacuum and the residue washed three times with toluene (5 mL) to clean unreacted btmgm from the product. After removal of all solvent traces under vacuum, [(κ²-N,N'-btmg)ZnCl₂] (279.9 mg, 0.57 mmol, 95%) was obtained as a white powder. Recrystallization from CH₃CN at –21 °C afforded colourless crystals suitable for X-ray diffraction. C₂₀H₃₀Cl₂N₆Zn (490.77): calcd. C 48.94, H 6.16, N 17.12, Cl 14.45, Zn 13.32; found C 48.95, H 6.21, N 17.19. ¹H NMR (400 MHz, CD₂Cl₂, 23 °C): δ = 7.46 (d, *J* = 8.14 Hz, 2 H, CH_{arom.}), 7.28 (dd, *J* = 7.55 Hz, 2 H), 6.32 (d, *J* = 7.36 Hz, 2 H, CH_{arom.}), 2.92 (m, 24 H, CH₃) ppm. ¹³C NMR (100.55 MHz, CD₂Cl₂, 296 K): δ = 165.57 (CN₃), 146.29 (C_{arom.}), 138.33 (C_{arom.}), 126.45 (C_{arom.}), 123.62 (C_{arom.}), 121.71 (C_{arom.}), 118.21 (C_{arom.}), 41.60, 40.35 (CH₃) ppm. IR: ν̄ = 3005 (w), 2952 (m), 2865 (m), 2789 (w), 1555 (s), 1527 (vs) 1467 (s), 1403 (vs), 1377 (s), 1332 (s), 1280 (m), 1233 (m), 1157 (s), 1108 (w), 1065 (m), 988 (s), 922 (w), 850 (w), 809 (m), 757 (m), 691 (m), 624 (w), 505 (w), 478 (w) cm^{–1}. HR-EI⁺: calcd. *m/z* = 490.1170 [C₂₀H₃₀N₆Cl₂Zn]⁺, exp. *m/z* = 490.1139 [M]⁺. EI⁺: *m/z* = 490.3 [M]⁺, 453.3 [M – Cl]⁺, 354.4 [btmg]⁺.

[(*n*Bu)₂Mg(κ²-N,N'-btmg)] (4): btmgm (103 mg, 0.29 mmol) was dissolved in toluene (5 mL). After addition of a (*n*Bu)₂Mg solution (0.3 mL, 1 M) in heptane by syringe at –20 °C, the clear yellow solution was stirred for an additional 10 min at –20 °C and a further 10 min at room temp. Pale yellow crystals were obtained by layering the solution with PE40/60 at –20 °C. ¹H NMR (200 MHz, [D₈]toluene, 298 K): δ = 7.40 (d, *J* = 7.65 Hz, 2 H, CH_{arom.}), 7.20 (t, *J* = 7.75, 1 Hz, 2 H, CH_{arom.}), 6.04 (d, *J* = 7.29 Hz, 2 H, CH_{arom.}), 2.40 (m, 24 H, CH₃), 2.09, 2.03, 1.77, 1.65, 1.56, 1.07, 0.3, 0.16, –0.45 (m, 19 H, butyl) ppm. ¹H NMR (200 MHz, C₆D₆, 303 K): δ = 7.43 (d, *J* = 7.58 Hz, 2 H, CH_{arom.}), 7.20 (t, *J* = 7.74, 1 Hz, 2 H, CH_{arom.}), 6.05 (d, *J* = 7.34 Hz, 2 H, CH_{arom.}), 2.31 (m, CH₃), 2.20–1.11 (butyl), 0.42, –0.3 (m, butyl) ppm. ¹³C NMR (100.56 MHz, C₆D₆, 296.9 K): δ = 165.26 (CN₃), 147.66, 138.31, 126.09, 122.93, 118.01 (C_{arom.}), 40.2, 39.3 (CH₃), 34.55, 32.66, 31.13, 25.13, 22.74, 15.33, 14.75, 13.93, 13.31 (coupling with ¹H signal at δ = 1.42), 10.4 (butyl) ppm. At low-temperature ¹H NMR (200 MHz, [D₈]toluene, 213 K) the CH₃ group resonances of the btmgm ligand split into four signals at 3.28 (s, 6 H), 2.39 (s, 6 H), 1.86 (s, 6 H), 1.66 (s, 6 H), and the signals from the butyl groups showed at 2.13, 1.92, 1.78, 1.48, 1.23, 1.19, 0.21, –0.28 (m, 20 H) ppm.

[(κ²-N,N'-btmg)MgBr₂] (5): The btmgm ligand (118 mg, 0.33 mmol) was dissolved in THF (15 mL). Then a solution of MeMgBr (0.22 mL, 0.66 mmol, 2 equiv., 3 M in Et₂O) was added dropwise by a syringe. The reaction mixture was stirred for 1.5 h at room temp. Colourless, cloudy crystals suitable for X-ray diffraction were obtained by layering the reaction mixture with PE 40/60. ¹H NMR (399.89 MHz, CD₂Cl₂, 294.6 K): δ = 7.46 (dd, *J* = 8.05, 0.65 Hz, 2 H, CH_{arom.}), 7.29 (t, *J* = 7.78 Hz, 2 H, CH_{arom.}), 6.31 (dd, *J* = 7.45, 0.86 Hz, 2 H, CH_{arom.}), 3.1–2.4 (br. s, 24 H, CH₃) ppm. ¹H NMR (200 MHz, CD₂Cl₂, 303 K): δ = 7.47 (d, *J* =

8.08 Hz, 2 H, CH_{arom.}), 7.29 (t, $J = 7.77$ Hz, 2 H, CH_{arom.}), 6.31 (d, $J = 7.35$ Hz, 2 H, CH_{arom.}), 2.92, 2.80 (br. s, 24 H, CH₃) ppm. ¹³C NMR (100.56 MHz, CD₂Cl₂, 296.0 K): $\delta = 165.98$ (CN₃), 145.75, 137.84, 126.06, 123.22, 121.87, 118.11 (C_{arom.}), 41.0, 40.00 (br., CH₃) ppm. The guanidino CH₃ group resonances were split at lower temperatures in the ¹H NMR (399.89 MHz, CD₂Cl₂, 243 K) spectra to give four signals at 3.29 (s, 6 H), 2.97 (s, 6 H), 2.80 (s, 6 H) and 2.18 (s, 6 H) ppm. MS (EI): m/z (%) = 538 (90) [M⁺], 459 (78) [M⁺ – Br⁻], 354 (96) [L⁺]. IR (KBr): $\tilde{\nu} = 2945$ (s), 2885 (s), 2789 (m), 1554 (vs), 1466 (s), 1403 (s), 1375 (s), 1336 (s), 1279 (m), 1234 (m), 1158 (s), 1109 (m), 1063 (m), 1022 (s), 922 (m), 875 (m), 848 (m), 808 (w), 768 (w), 693 (w), 623 (w) cm⁻¹.

[(κ²-N,N'-btmgn)MgCl₂]: A solution of tmgn (103 mg, 0.29 mmol) in THF_{abs.} (10 mL) was prepared and CH₃CH₂MgCl (0.29 mL, 0.58 mmol, 2 equiv., 2 M in THF) added with a syringe at room temp. over a period of 1 h. After removal of the solvent one obtains the product (200 mg) in the form of a white powder. ¹H NMR (399.89 MHz, CD₂Cl₂, 295 K): $\delta = 7.46$ (d, $J = 8.00$ Hz, 2 H, CH_{arom.}), 7.28 (t, $J = 7.77$ Hz, 2 H, CH_{arom.}), 6.31 (d, $J = 7.38$ Hz, 2 H, CH_{arom.}), 3.2–2.4 (br. s, 24 H, CH₃) ppm. ¹H NMR (200 MHz, CD₂Cl₂, 303 K): $\delta = 7.46$ (d, $J = 8.10$ Hz, 2 H, CH_{arom.}), 7.29 (t, $J = 7.70$ Hz, 2 H, CH_{arom.}), 6.32 (d, $J = 7.37$ Hz, 2 H, CH_{arom.}), 2.92, 2.82 (br. s, 24 H, CH₃) ppm. ¹³C NMR (100.56 MHz, CD₂Cl₂, 296.5 K): $\delta = 165.64$ (CN₃), 145.85, 137.85, 126.03, 123.14, 121.90, 118.06 (C_{arom.}), 41.0, 39.66 (br., CH₃) ppm. MS (EI): m/z (%) = 448 (43) [M⁺], 354 (98) [L⁺]. IR (KBr): $\tilde{\nu} = 2952$ (s), 2873 (s), 2794 (sh), 1547 (vs), 1536 (vs), 1466 (s), 1401 (vs), 1335 (s), 1280 (m), 1234 (m), 1137 (s), 1063 (m), 1018 (m), 996 (m), 923 (w), 887 (w), 808 (w), 764 (w), 692 (w), 623 (w) cm⁻¹.

[Ph₂Mg(κ²-N,N'-btmgn)] (6): A solution of Ph₂Mg·3THF (201 mg, 0.51 mmol, 1.5 equiv.) and btmgn (120 mg, 0.34 mmol) in THF (10 mL) was stirred for 2 h at room temp. After layering the reaction mixture with PE 40/60 and addition of an excess of Ph₂Mg·3THF at –20 °C colourless, slightly cloudy crystals suitable for X-ray diffraction were obtained. In addition the free btmgn ligand crystallized in the form of colourless and clear crystals. The solvent was removed under vacuum and the remaining colourless solid washed three times with PE 40/60 to obtain the product (258 mg, 0.49 mmol, 95% yield). ¹H NMR (200 MHz, C₆D₆, 303 K): $\delta = 8.16$ (d, $J = 7.31$ Hz, 4 H, CH_{arom.}), 7.48–7.18 (m, 10 H, Ph), 6.09 (d, $J = 7.31$ Hz, 2 H, CH_{arom.}), 2.51 (m, 12 H, CH₃), 1.85 (s, 12 H, CH₃) ppm. ¹³C NMR (100.56 MHz, C₆D₆, 296.3 K): $\delta = 165.03$ (CN₃), 147.59, 141.19, 138.44, 129.02, 128.55, 126.18, 126.13, 124.18, 123.13, 118.05 (C_{arom.}), 38.89, 36.3 (br., CH₃) ppm. ¹H NMR (200 MHz, [D₈]THF, 303 K): $\delta = 7.61$ (m, 4 H, CH_{arom.}), 7.41 (d, $J = 7.91$ Hz, 2 H, CH_{arom.}), 7.22–7.17 (m, 2 H, CH_{arom.}), 6.8 (m, 6 H, CH_{arom.}), 6.32 (d, $J = 7.14$ Hz, 2 H, CH_{arom.}), 2.89–2.26 (m, 24 H, CH₃) ppm. The btmgn CH₃ group resonances were split in the ¹H NMR (200 MHz, [D₈]THF, 233 K) spectrum at lower temperatures into four signals located at 3.03 (s, 6 H), 2.76 (s, 6 H), 2.34 (s, 6 H) and 2.10 (s, 6 H) ppm. ¹H NMR (200 MHz, [D₈]toluene, 298 K): $\delta = 8.03$ (m, 4 H, CH_{arom.}), 7.5–7.2 (m, 10 H, Ph), 6.06 (m, 2 H, CH_{arom.}), 2.85–2.34 (m, 12 H, CH₃), 1.91 (br. s, 12 H, CH₃) ppm. Again splitting of the signal due to the btmgn CH₃ groups in the ¹H NMR (200 MHz, [D₈]toluene, 223 K) spectra was observed leading to four signals at 2.95 (s, 6 H), 1.95 (s, 6 H), 1.80 (s, 6 H) and 1.72 (s, 6 H) ppm.

[Ph₂Mg(κ²-N,N'-btmgb)] (7): A solution of Ph₂Mg·3THF (119 mg, 0.30 mmol, 1.6 equiv.) and btmgn (58 mg, 0.19 mmol) in THF (6 mL) was stirred for 2 h at room temp. After removal of the solvent under vacuum the beige residue was washed three times with PE 40/60 to obtain the product (77 mg, 0.16 mmol, 85% yield).

In addition, colourless and clear crystals of the free btmgb ligand precipitated. C₂₈H₃₈MgN₆·THF (627.15): calcd. C 69.24, H 8.35, N 15.14; found C 63.61, H 8.14, N 15.94. ¹H NMR (399.89 MHz, C₆D₆, 295 K): $\delta = 8.27$ (m, 4 H, CH_{arom.}), 7.51 (t, $J = 7.25$ Hz, 4 H, CH_{arom.}), 7.39 (t, $J = 7.24$ Hz, 2 H, CH_{arom.}), 6.90 (dd, $J = 5.88$, 3.47 Hz, 2 H, CH_{arom.}), 6.42 (dd, $J = 5.87$, 3.49 Hz, 2 H, CH_{arom.}), 2.84 (m, 6 H, CH₃), 1.96 (br. s, 18 H, CH₃) ppm. ¹³C NMR (100.56 MHz, C₆D₆, 296.5 K): $\delta = 142.07$, 141.33, 129.02, 128.55, 126.28, 124.41, 122.07, 120.29 (C_{arom.}), 39.51 (CH₃) ppm. ¹H NMR (200 MHz, [D₈]toluene, 298 K): $\delta = 8.11$ (m, 4 H), 7.5–7.2 (m, 6 H), 6.85 (m, 2 H), 6.39 (m, 2 H), 2.98–1.83 (m, 24 H, CH₃) ppm. At lower temperatures (193 K, 200 MHz, [D₈]THF, ¹H NMR) the signals arising from the btmgb ligand CH₃ groups split into four signals at 2.92 (s, 6 H), 1.97 (s, 6 H), 1.84 (s, 6 H) and 1.78 (s, 6 H) ppm.

[H₂O(C₂H₅)₂][B(C₆F₅)₄]: The preparation followed the procedure described in the literature.^[36] However, instead of crystallization of the product, the solvent was removed under vacuum and the solid residue dissolved in CH₂Cl₂ was filtered through silica. Starting with LiB(C₆F₅)₄·2.5C₂H₅OC₂H₅ (305.4 mg), aqueous HCl (1.5 mL, 2 M) in Et₂O and Et₂O (6 mL), we obtained the product (287 mg, 90%) in the form of a pale yellow oil.

[btmgnH][B(C₆F₅)₄]: A solution of [H(OEt₂)₂][B(C₆F₅)₄] (149 mg, 0.18 mmol) in CH₃CN (3 mL) was added by syringe to a solution of btmgn (65 mg, 0.18 mmol) in CH₃CN (3 mL). The colourless clear reaction mixture was stirred for 2 h at room temp. After removal of the solvent under vacuum the beige solid residue was washed three times with PE 40/60 leading to the product (156 mg, 0.15 mmol, 84%) in the form of a beige solid foam. ¹H NMR (399.89 MHz, CD₂Cl₂, 295.6 K): $\delta = 15.02$ (s, 1 H, H⁺), 7.46 (d, $J = 8.08$ Hz, 2 H, CH_{arom.}), 7.36 (t, $J = 7.67$ Hz, 2 H, CH_{arom.}), 6.43 (d, $J = 7.24$ Hz, 2 H, CH_{arom.}), 2.90 (s, 24 H, CH₃) ppm. ¹³C NMR (100.56 MHz, CD₂Cl₂, 295.6 K): $\delta = 159.32$ (CN₃), 141.64, 135.07, 126.27, 122.72, 113.90 (C_{arom.}), 40.10 (CH₃) ppm. ¹¹B NMR (128.30 MHz, CD₂Cl₂, 295.6 K): $\delta = -16.66$ (s) ppm. ¹⁹F NMR (376.27 MHz, CD₂Cl₂, 295.6 K): $\delta = -133.11$ (m), –163.72 (t, $J = 20.37$ Hz), –167.60 (t, $J = 18.52$ Hz) ppm. MS (ESI, CH₂Cl₂): m/z (%) = 355.26 (100) [M]⁺.

[btmgbH][B(C₆F₅)₄]: A solution of [H(OEt₂)₂][B(C₆F₅)₄] (197 mg, 0.24 mmol) in Et₂O (5 mL) was added by syringe to a solution of btmgb (73 mg, 0.24 mmol) in Et₂O (5 mL). The colourless clear solution was stirred for 2 h at room temp. After removal of the solvent under vacuum the white solid obtained was washed three times with PE 40/60 yielding the product (220 mg, 0.22 mmol) in the form of a colourless foam (93% yield). C₄₀H₂₉BF₂₀N₆ (984.47): calcd. C 48.80, H 2.97, N 8.54; found C 47.71, H 3.49, N 7.73. ¹H NMR (399.89 MHz, CD₂Cl₂, 295.6 K): $\delta = 6.96$ (dd, $J = 5.92$, 3.46 Hz, 2 H, CH_{arom.}), 6.58 (dd, $J = 5.92$, 3.48 Hz, 2 H, CH_{arom.}), 2.86 (s, 24 H, CH₃) ppm. ¹³C NMR (100.56 MHz, CD₂Cl₂, 295.6 K): $\delta = 159.46$ (CN₃), 134.77, 123.12, 119.10, (C_{arom.}) 39.88 (CH₃) ppm. ¹¹B NMR (128.30 MHz, CD₂Cl₂, 295.6 K): $\delta = -16.67$ (s) ppm. ¹⁹F NMR (376.27 MHz, CD₂Cl₂, 295.6 K): $\delta = -133.13$ (m), –163.74 (t, $J = 20.40$ Hz), –167.60 (t, $J = 18.10$ Hz) ppm. IR (KBr): $\tilde{\nu} = 2938$ (m), 2878 (sh), 1643 (m), 1535 (vs), 1464 (vs), 1391 (s), 1273 (m), 1149 (m), 1090 (s), 1026 (m), 980 (vs), 752 (m), 663 (m), 559 (w) cm⁻¹.

[Me₂Al(κ²-N,N'-btmgn)][B(C₆F₅)₄]: [(btmgnH)B(C₆F₅)₄] (156 mg, 0.15 mmol) was dissolved in toluene (5–10 mL). After dropwise addition of a Me₂Al solution (0.15 mL, 2 M) in toluene, the colourless clear reaction mixture was stirred for a period of 2 h at room temperature. Subsequently the solvent was removed in vacuo leaving a colourless solid, which was washed three times with PE 40/60. Yield

150 mg (0.14 mmol, 93%). ^1H NMR (399.89 MHz, CD_2Cl_2 , 295.7 K): δ = 7.64 (d, J = 8.15 Hz, 2 H, $\text{CH}_{\text{arom.}}$), 7.40 (t, J = 7.83 Hz, 2 H, $\text{CH}_{\text{arom.}}$), 6.44 (d, J = 7.35 Hz, 2 H, $\text{CH}_{\text{arom.}}$), 2.98 (s, 12 H, CH_3), 2.77 (m, 12 H, CH_3), -0.87 (s, 6 H, Al-CH_3) ppm. ^{13}C NMR (100.56 MHz, CD_2Cl_2 , 297.3 K): δ = 165.65 (CN_3), 149.44, 147.04, 140.82, 139.53, 137.30, 135.28, 129.04, 128.23, 126.71, 125.07, 120.47, 117.94 ($\text{C}_{\text{arom.}}$), 41.30, 40.05 (CH_3), -11.45 (Al-CH_3) ppm. ^{11}B NMR (128.30 MHz, CD_2Cl_2 , 295.9 K): δ = -16.65 (s) ppm. ^{19}F NMR (376.23 MHz, CD_2Cl_2 , 295.9 K): δ = -133.07 (m), -163.66 (t, J = 20.41 Hz), -167.53 (t, J = 17.24 Hz) ppm. MS (FAB): m/z (%) = 411 (100) [M^+], 355 (28) [btmgnH $^+$].

[Me₂Al(κ^2 -*N,N'*-btmgn)]PF₆]: A solution of Me₃Al in toluene (2 mL, 0.46 mmol, 0.92 mmol, 3.3 equiv.) was added dropwise to a solution of [(btmgnH)PF₆] (140 mg, 0.28 mmol) (prepared as described in the literature, see ref.^[19]) in THF (50 mL). The reaction mixture was stirred for 20 h at room temp. The solvent was removed under vacuum and the residue was washed several times with toluene to obtain [Me₂Al(κ^2 -*N,N'*-btmgn)]PF₆] in 128 mg (0.23 mmol, 82%) yield. ^1H NMR (399.89 MHz, 295 K, CD_2Cl_2): δ = 7.61 (d, J = 7.74 Hz, 2 H, $\text{CH}_{\text{arom.}}$), 7.41 (t, J = 7.30 Hz, 2 H, $\text{CH}_{\text{arom.}}$), 6.47 (d, J = 7.02 Hz, 2 H, $\text{CH}_{\text{arom.}}$), 3.01 (s, 12 H, CH_3), 2.78 (br. s, 12 H, CH_3), -0.88 (s, 6 H) ppm. ^{13}C NMR (100.56 MHz, 296.7 K, CD_2Cl_2): δ = 165.53, 159.23 (CN_3), 142.12, 141.02, 137.17, 126.69, 126.21, 124.71, 122.16, 120.45, 117.90, 113.69, ($\text{C}_{\text{arom.}}$), 41.31, 40.04 (CH_3), -11.43 (br., Al-CH_3) ppm. ^{19}F NMR (376.23 MHz, CD_2Cl_2 , 193.4 K): δ = -72.7 (d). ^{31}P NMR (242.92 MHz, 295 K, CD_3CN): δ = -144.64 [sept, $J(^{31}\text{P},^{19}\text{F})$ = 706.3 Hz] ppm. Low-temperature ^1H NMR (399.89 MHz, CD_2Cl_2 , 193.4 K) shows the splitting of the btmgn CH_3 groups [3.11 (s, 6 H), 2.98 (s, 6 H), 2.90 (s, 6 H), 2.25 (s, 6 H)] and of the CH_3 groups at the Al [-0.98 (s, 3 H), -1.00 (s, 3 H)].

[Me₂Al(κ^2 -*N,N'*-btmgn)]B(C₆H₅)₄, 8[B(C₆H₅)₄]: A solution of Me₃Al (2 mL) in toluene (0.46 mL, 0.92 mmol, 3.3 equiv.) was added dropwise to a solution of [(btmgnH)PF₆] (140 mg, 0.28 mmol) (prepared as described in the literature, see ref.^[19]) in 50 mL THF. The reaction mixture was stirred for 20 h at room temp. The solvent was removed under vacuum and the residue washed several times with toluene to obtain [Me₂Al(κ^2 -*N,N'*-btmgn)]PF₆] in 128 mg (0.23 mmol, 82%) yield. Then a solution of [Me₂Al(κ^2 -*N,N'*-btmgn)]PF₆] in THF (50 mL) was prepared, NaBPh₄ (79 mg, 0.23 mmol) was added and the mixture was stirred for 1 h at room temp. The solution was filtered through silica and the filtrate concentrated. Colourless crystals were obtained from the THF solution layered by *n*-hexane. C₄₆H₅₆AlBN₆ (730.76): calcd. C 75.60, H 7.72, N 11.50; found C 75.60, H 7.70, N 10.93. ^1H NMR (399.89 MHz, CD_2Cl_2): δ = 7.64 (d, J = 8.3 Hz, 2 H, $\text{CH}_{\text{arom.}}$), 7.47–7.36 (m, 2 H, $\text{CH}_{\text{arom.}}$), 7.32 (m, 8 H, $\text{CH}_{\text{arom.}}$), 7.02 (t, J = 7.4 Hz, 8 H, $\text{CH}_{\text{arom.}}$), 6.87 (t, J = 7.2 Hz, 4 H, $\text{CH}_{\text{arom.}}$), 6.41 (d, J = 7.5 Hz, 2 H, $\text{CH}_{\text{arom.}}$), 2.91 (s, 12 H, CH_3), 2.73 (br. s, 12 H, CH_3), -0.88 (s, 6 H) ppm. ^{13}C NMR (100.56 MHz, CD_2Cl_2): δ = 165.54 (CN_3), 164.82, 164.33, 163.84, 163.35 (BPh₄) 140.81, 137.26, 135.96, 126.73, 125.70, 125.02, 121.79, 117.90, 113.84 ($\text{C}_{\text{arom.}}$), 41.42, 40.14 (CH_3), -11.79 (br., Al-CH_3) ppm. MS (ESI): m/z (%) = 411 (100) [M^+]. IR (CsI): $\tilde{\nu}$ = 3041 (w), 2945 (m), 2913 (sh), 2807 (w), 1583 (vs), 1529 (vs), 1474 (s), 1411 (s), 1381 (s), 1318 (s), 1235 (m), 1169 (s), 1154 (w), 1069 (m), 1023 (m), 1009 (m), 865 (vs), 840 (vs), 771 (s), 706 (m), 675 (s), 558 (s), 512 (m) cm^{-1} .

[Me₂Al(κ^2 -*N,N'*-btmgb)]B(C₆F₅)₄]: [(btmgbH)B(C₆F₅)₄] (197 mg, 0.20 mmol) was dissolved in toluene (20 mL). A Me₃Al solution (2 mL) in toluene (0.2 mL, 0.4 mmol) was added dropwise by syringe. The colourless clear solution was stirred for 1 h at room temp. After removal of the solvent under vacuum a colourless residue was

obtained, which was washed three times with PE 40/60 to yield the product together with approx. equimolar amounts of toluene (220 mg, 0.194 mmol, 97% yield). ^1H NMR (399.89 MHz, CD_2Cl_2 , 295.9 K): δ = 7.03 (dd, J = 5.94, 1 Hz, 2 H, $\text{CH}_{\text{arom.}}$), 6.61 (dd, J = 5.93, 3.43 Hz, 2 H, $\text{CH}_{\text{arom.}}$), 2.98 (s, 12 H, CH_3), 2.78 (m, 12 H, CH_3), -0.77 (s, 6 H) ppm. ^{13}C NMR (100.56 MHz, CD_2Cl_2 , 297.2 K): δ = 163.31 (CN_3), 149.37, 147.04, 137.41, 135.10, 124.20, 119.17 ($\text{C}_{\text{arom.}}$), 40.71, 39.85 (CH_3), -10.2 (Al-CH_3) ppm. ^{11}B NMR (128.30 MHz, CD_2Cl_2 , 295.9 K): δ = -16.67 (s) ppm. ^{19}F NMR (376.23 MHz, CD_2Cl_2 , 295.9 K): δ = -133.12 (m), -163.73 (t, J = 20.39 Hz), -167.58 (t, J = 17.76 Hz) ppm. MS (FAB): m/z (%) = 305 (100) [btmgbH $^+$]. IR (KBr): $\tilde{\nu}$ = 2952 (s), 2883 (sh), 1642 (s), 1562 (s), 1529 (s), 1464 (vs), 1413 (s), 1333 (m), 1273 (m), 1089 (s), 980 (s), 834 (m), 754 (m), 681 (m) cm^{-1} .

[(κ^2 -*N,N'*-btmgn)GaCl₂][GaCl₄]-THF (9): A solution of GaCl₃ (104 mg, 0.59 mmol) in THF (5 mL) was added dropwise by syringe to a solution of btmgn (118 mg, 0.33 mmol) in THF (5 mL) at -78 °C. After stirring the reaction mixture for 30 min it was warmed to room temperature and the solvent was removed under vacuum. The residue was washed twice with toluene. After removal of all solvent traces under vacuum [(κ^2 -*N,N'*-btmgn)GaCl₂][GaCl₄] (151 mg, 0.19 mmol, 66%) (containing traces of solvent and protonated ligand) was obtained as a white powder. C₂₄H₃₈Cl₆Ga₂N₆O (778.74): calcd. C 37.02, H 4.92, Cl 27.32, Ga 17.9, N 10.79; found C 34.26, H 4.31, N 11.58. Crystallization from THF afforded colourless crystals suitable for XRD. ^1H NMR (399.89 MHz, CD_2Cl_2 , 296 K): δ = 7.77 (d, J = 8 Hz, 2 H, $\text{CH}_{\text{arom.}}$), 7.52 (t, J = 8 Hz, 2 H, $\text{CH}_{\text{arom.}}$), 6.49 (d, J = 7.6 Hz, 2 H, $\text{CH}_{\text{arom.}}$), 3.13 (s, 12 H, CH_3), 2.93 (s, 12 H, CH_3) ppm. ^{13}C NMR (100.56 MHz, CD_2Cl_2 , 296 K): δ = 164.36 (CN_3), 139.74 (arom. C), 137.87 (arom. C), 127.31 (arom. C), 126.58 (arom. C), 119.0 (arom. C), 42.12 (CH_3), 41.02 (CH_3) ppm. IR (CsI): $\tilde{\nu}$ = 2940 (m), 1958 (m), 1410 (s), 1311 (vs), 1157 (s), 1016 (s), 869 (s), 820 (vs), 762 (vs), 629 (m), 507 (m) cm^{-1} . MS (FAB+): m/z (%) = 495.2 (30) [M^+ - GaCl₄ - THF].

X-ray Crystallographic Study: Suitable crystals were taken directly out of the mother liquor, immersed in perfluorinated polyether oil and fixed on top of a glass capillary. Intensity measurements were made at low temperature on Nonius Kappa CCD (complexes **1–3** and **5–8** at 200 K) and Bruker AXS Smart 1000 diffractometers (complex **4** at 100 K) (Mo- K_α radiation, graphite monochromator, λ = 0.71073 Å). The data collected were processed with the standard Nonius^[37] or Bruker^[38] software. The structures were solved by conventional direct methods^[37] (complexes **1–3** and **5–8**) or by direct methods with dual-space recycling (“Shake-and-Bake”)^[39] (complex **4**). Because of severe disorder and unresolvable composition, electron density attributed to solvent of crystallization (alkanes from petroleum ether) was removed from the structure (and the corresponding F_{obs}) of **4** with the BYPASS procedure,^[40] as implemented in PLATON (SQUEEZE).^[41] Restraints had to be applied to the bond lengths and the adps of the carbon atoms of the *n*-butyl groups in **4**. All further calculations were performed using the SHELXTL-PLUS software package. Graphical handling of the structural data during solution and refinement was performed with XPMA.^[42] Structural representations were generated using Winray 32.^[43] Atomic coordinates and anisotropic thermal parameters of non-hydrogen atoms were refined by full-matrix least-squares calculations. Table 1 contains some information on the crystals of the btmgn complexes.

CCDC-732382 (for **8**), -732383 (for **4**), -732384 (for **3**), -732385 (for **1**), -732386 (for **2**), -732387 (for **5**), -732388 (for **6**) and -734798 (for **9**) contain the supplementary crystallographic data for

Table 1. Crystal data and refinement details for complexes 1–9.

	1	2	3	4
Formula	C ₂₀ H ₃₈ N ₆ Zn	C ₂₄ H ₄₀ N ₆ Zn·0.75C ₄ H ₈ O	C ₂₀ H ₃₀ Cl ₂ N ₆ Zn	C ₂₈ H ₄₈ MgN ₆
<i>M_r</i> [g mol ⁻¹]	427.93	532.07	490.77	493.03
Crystal size [mm]	0.50 × 0.40 × 0.40	0.40 × 0.35 × 0.30	0.20 × 0.15 × 0.15	0.26 × 0.24 × 0.05
Crystal system	P $\bar{1}$	P2 ₁ /c	P2 ₁ /c	P $\bar{1}$
Space group	triclinic	monoclinic	monoclinic	triclinic
<i>a</i> [Å]	8.4230(17)	14.959(3)	11.288(2)	10.9961(16)
<i>b</i> [Å]	9.0370(18)	10.988(2)	11.438(2)	11.4850(17)
<i>c</i> [Å]	17.103(3)	18.961(4)	17.965(4)	14.087(2)
α [°]	92.57(3)			95.632(3)
β [°]	102.49(3)	108.37(3)	94.56(3)	110.202(3)
γ [°]	116.77(3)			101.911(3)
<i>V</i> [Å ³]	1119.5(4)	2957.7(10)	2312.2(8)	1605.6(4)
$\rho_{\text{calcd.}}$ [g cm ⁻³]	1.269	0.858	1.410	1.020
<i>Z</i>	2	4	4	2
<i>F</i> (000)	460	1144	1024	540
<i>hkl</i> range	-12 ≤ <i>h</i> ≤ 12 -13 ≤ <i>k</i> ≤ 13 -26 ≤ <i>l</i> ≤ 26	-21 ≤ <i>h</i> ≤ 21 -15 ≤ <i>k</i> ≤ 15 -26 ≤ <i>l</i> ≤ 26	-15 ≤ <i>h</i> ≤ 15 -16 ≤ <i>k</i> ≤ 16 -25 ≤ <i>l</i> ≤ 25	-13 ≤ <i>h</i> ≤ 12 -13 ≤ <i>k</i> ≤ 13 0 ≤ <i>l</i> ≤ 16
θ range [°]	1.24–33.10	1.43–30.00	1.81–30.01	1.84–25.12
μ [mm ⁻¹]	1.113	0.858	1.312	0.079
Measured reflections	15634	54801	64545	26784
Unique reflections (<i>R</i> _{int})	8472 (0.0285)	8622 (0.0705)	6738 (0.0676)	5710 (0.0448)
Observed reflections [<i>I</i> > 2σ(<i>I</i>)]	8472	8622	6738	3527
Refined parameters/restraints	254/0	317/0	270/0	326/16
Goodness-of-fit	1.075	1.068	0.965	1.148
<i>R</i> ₁ [<i>I</i> > 2σ(<i>I</i>)]	0.0365	0.0512	0.0436	0.0753
<i>wR</i> ₂ (all data)	0.1008	0.1544	0.1055	0.2479
Residual electron density [e Å ⁻³] (max./min.)	0.463/–0.472	1.251/–0.407	0.617/–0.473	1.009/–0.488
	5	6	8	9
Formula	C ₂₀ H ₃₀ Br ₂ MgN ₆	C ₃₂ H ₄₀ MgN ₆ ·C ₄ H ₈ O	C ₄₆ H ₅₆ AlBN ₆	C ₂₀ H ₃₀ Cl ₆ Ga ₂ N ₆ ·C ₄ H ₈ O
<i>M_r</i> [g mol ⁻¹]	538.63	605.11	730.76	778.74
Crystal size [mm]	0.40 × 0.20 × 0.20	0.50 × 0.40 × 0.20	0.15 × 0.15 × 0.07	0.25 × 0.20 × 0.20
Crystal system	P2 ₁ /c	P2 ₁ /c	<i>Pbcm</i>	P2 ₁ /n
Space group	monoclinic	monoclinic	orthorhombic	monoclinic
<i>a</i> [Å]	11.445(2)	20.101(4)	9.0443(9)	17.291(4)
<i>b</i> [Å]	11.678(2)	10.145(2)	16.9810(17)	10.310(2)
<i>c</i> [Å]	18.167(4)	17.502(4)	27.639(3)	18.968(4)
α [°]				
β [°]	93.25(3)	109.47(3)		98.84(3)
γ [°]				
<i>V</i> [Å ³]	2424.2(8)	3365.1(12)	4244.8(7)	3341.3(12)
$\rho_{\text{calcd.}}$ [g cm ⁻³]	1.476	1.194	1.143	1.548
<i>Z</i>	4	4	4	4
<i>F</i> (000)	1096	1304	1568	1584
<i>hkl</i> range	-15 ≤ <i>h</i> ≤ 16 -16 ≤ <i>k</i> ≤ 16 -24 ≤ <i>l</i> ≤ 25	-28 ≤ <i>h</i> ≤ 28 -14 ≤ <i>k</i> ≤ 14 -24 ≤ <i>l</i> ≤ 24	0 ≤ <i>h</i> ≤ 10 0 ≤ <i>k</i> ≤ 20 0 ≤ <i>l</i> ≤ 32	-23 ≤ <i>h</i> ≤ 23 -14 ≤ <i>k</i> ≤ 14 -26 ≤ <i>l</i> ≤ 26
θ range [°]	1.78 to 30.22	2.15–30.01	2.25–25.01	2.17–29.58
μ [mm ⁻¹]	3.388	0.090		2.121
Measured reflections	48743	19457	71870	18664
Unique reflections (<i>R</i> _{int})	7140 (0.1057)	9818 (0.0696)	3832 (0.0987)	9359 (0.0720)
Observed reflections [<i>I</i> > 2σ(<i>I</i>)]	7140	9818	2591	9359
Refined parameters/restraints	270/0	405/0	256/0	360/0
Goodness-of-fit	1.014	1.022	1.086	1.019
<i>R</i> ₁ [<i>I</i> > 2σ(<i>I</i>)]	0.0496	0.0592	0.0643	0.0473
<i>wR</i> ₂ (all data)	0.1338	0.1392	0.1691	0.1095
Residual electron density [e Å ⁻³] (max./min.)	0.757/–1.399	0.287/–0.271	0.813/–0.667	0.775/–0.744

this paper. These data can be obtained free of charge from The Cambridge Crystallographic Data Centre via www.ccdc.cam.ac.uk/data_request/cif.

Quantum Chemical Calculations: DFT calculations were carried out with the help of the TURBOMOLE program.^[44] The BP86

functional^[45] in combination with an SV(P) basis set^[46] was applied.

Supporting Information (see also the footnote on the first page of this article): Selected structural parameters of **1–8**, selected IR spectra, VT-NMR spectra for **3** (–30 to +60 °C) and structures of the

possible products of intramolecular alkyl transfer reactions starting with a model bisguanidine dialkyl Zn complex. Quantum chemical (DFT) calculations on the activation of Cp_2TiMe_2 by methyl transfer to $[(\kappa^2\text{-N,N'-btmgn})\text{AlMe}_2]^+$.

Acknowledgments

Continuous financial support from the Deutsche Forschungsgemeinschaft (DFG) is gratefully acknowledged.

- [1] D. A. Atwood, *Coord. Chem. Rev.* **1998**, *176*, 407–430, and references cited therein.
- [2] S. Dagorne, D. A. Atwood, *Chem. Rev.* **2008**, *108*, 4037–4071.
- [3] C. Dohmeier, H. Schnöckel, C. Robl, U. Schneider, R. Ahlrichs, *Angew. Chem.* **1993**, *105*, 1714–1716; *Angew. Chem. Int. Ed. Engl.* **1993**, *32*, 1655–1657.
- [4] a) M. Bochmann, D. M. Dawson, *Angew. Chem.* **1996**, *108*, 2371–2373; *Angew. Chem. Int. Ed. Engl.* **1996**, *35*, 2226–2228; b) C. T. Burns, D. S. Stelck, P. J. Shapiro, A. Vij, K. Kunz, G. Kehr, T. Concolino, A. L. Rheingold, *Organometallics* **1999**, *18*, 5432–5434; c) M. Huber, A. Kurek, I. Krossing, R. Mühlhaupt, H. Schnöckel, *Z. Anorg. Allg. Chem.* **2009**, *635*, in press (DOI: 10.1002/zaac.200801378).
- [5] M. Bochmann, M. J. Sarsfield, *Organometallics* **1998**, *17*, 5908–5912.
- [6] K.-C. Kim, C. A. Reed, G. S. Long, A. Sen, *J. Am. Chem. Soc.* **2002**, *124*, 7662–7663.
- [7] J. D. Young, M. A. Kahn, R. J. Wehmschulte, *Organometallics* **2004**, *23*, 1965–1967.
- [8] M. P. Coles, R. F. Jordan, *J. Am. Chem. Soc.* **1997**, *119*, 8125–8126.
- [9] G. Talarico, V. Barone, P. H. M. Budzelaar, C. Adamo, *J. Phys. Chem. A* **2001**, *105*, 9014–9023.
- [10] A. V. Korolev, E. Ihara, I. A. Guzei, V. G. Young Jr., R. F. Jordan, *J. Am. Chem. Soc.* **2001**, *123*, 8291–8309.
- [11] S. Dagorne, L. Lavanant, R. Welter, C. Chassenieux, P. Haquette, G. Jaouen, *Organometallics* **2003**, *22*, 3732–3741.
- [12] D. Pappalardo, C. Tedesco, C. Pellecchia, *Eur. J. Inorg. Chem.* **2002**, 621–628.
- [13] See, for example: Y. Sarazin, M. Schormann, M. Bochmann, *Organometallics* **2004**, *23*, 3296–3302; and references given therein.
- [14] R. Schwesinger, *Nachr. Chem. Tech. Lab.* **1990**, *38*, 1214–1226; and references given therein.
- [15] F. T. Edelmann, *Adv. Organomet. Chem.* **2008**, *57*, 183–352.
- [16] a) J. Börner, S. Herres-Pawlis, U. Flörke, K. Huber, *Eur. J. Inorg. Chem.* **2007**, 5645–5651; b) J. Börner, U. Flörke, K. Huber, A. Döring, D. Kuckling, S. Herres-Pawlis, *Chem. Eur. J.* **2009**, *15*, 2362–2376.
- [17] a) R. Dinda, O. Ciobanu, H. Wadepohl, O. Hübner, R. Acharaya, H.-J. Himmel, *Angew. Chem.* **2007**, *119*, 9270–9273; *Angew. Chem. Int. Ed.* **2007**, *46*, 9110–9113; b) O. Ciobanu, D. Emeljanenko, E. Kaifer, H.-J. Himmel, *Inorg. Chem.* **2008**, *47*, 4774–4778.
- [18] U. Wild, O. Hübner, A. Maronna, M. Enders, E. Kaifer, H. Wadepohl, H.-J. Himmel, *Eur. J. Inorg. Chem.* **2008**, 4440–4447.
- [19] V. Raab, J. Kipke, R. M. Gschwind, J. Sundermeyer, *Chem. Eur. J.* **2002**, *8*, 1682–1693.
- [20] A. Peters, U. Wild, O. Hübner, E. Kaifer, H.-J. Himmel, *Chem. Eur. J.* **2008**, *14*, 7813–7821.
- [21] J. Krahmer, R. Beckhaus, W. Saak, D. Haase, *Z. Anorg. Allg. Chem.* **2008**, *634*, 1696–1702.
- [22] P. C. Andrews, C. L. Raston, B. W. Skelton, A. H. White, *Organometallics* **1998**, *17*, 779–782.
- [23] a) M. Kaupp, H. Stoll, H. Preuss, W. Kaim, T. Stahl, G. van Koten, E. Wissing, W. J. J. Smeets, A. L. Spek, *J. Am. Chem. Soc.* **1991**, *113*, 5606–5618; b) E. Wissing, S. van der Linden, E. Rijnberg, J. Boersma, W. J. J. Smeets, A. L. Spek, G. van Koten, *Organometallics* **1994**, *13*, 2602–2608.
- [24] J. Lewiński, K. Suwała, M. Kubisiak, Z. Ochal, I. Juszyński, J. Lipkowski, *Angew. Chem.* **2008**, *120*, 8006–8009; *Angew. Chem. Int. Ed.* **2008**, *47*, 7888–7891.
- [25] K.-i. Yamada, H. Fujihara, Y. Yamamoto, Y. Miwa, T. Taga, K. Tomioka, *Org. Lett.* **2002**, *4*, 3509–3511.
- [26] D. Margetić, W. Nakanishi, T. Kumamoto, T. Ishikawa, *Heterocycles* **2007**, *71*, 2639–2658.
- [27] W. Nakanishi, T. Ishikawa, D. Margetić, *Bull. Chem. Soc. Jpn.* **2007**, *80*, 1187–1193.
- [28] H. Tang, H. G. Richey, *Organometallics* **2001**, *20*, 1569–1574.
- [29] P. J. A. Sáez, S. H. Oakley, M. P. Coles, P. B. Hitchcock, *Chem. Commun.* **2007**, 816–818.
- [30] S. Dagorne, S. Bellemin-Laponnaz, R. Welter, *Organometallics* **2004**, *23*, 3053–3061.
- [31] J. D. Masuda, D. W. Stephan, *Dalton Trans.* **2006**, 2089–2097.
- [32] J. A. C. Clyburne, R. D. Culp, S. Kamepalli, A. H. Cowley, A. Decken, *Inorg. Chem.* **1996**, *35*, 6651–6655.
- [33] P. Roquette, A. Maronna, A. Peters, E. Kaifer, H.-J. Himmel, Ch. Hauf, V. Herz, E.-W. Scheidt, W. Scherer, *Chem. Eur. J.* **2009**, submitted for publication.
- [34] See, for example, the recent work with *O,P*-phosphanylphenolate ligands: M. Haddad, M. Laghzaoui, R. Welter, S. Dagorne, *Organometallics* **2009**, *28*, 4584–4592.
- [35] M. Findeisen, T. Brand, S. Berger, *Magn. Reson. Chem.* **2007**, *45*, 175–178.
- [36] P. Jutzi, C. Müller, A. Stämmler, H.-G. Stämmler, *Organometallics* **2000**, *19*, 1442–1444.
- [37] DENZO-SMN, Data processing software, Nonius, **1998**; <http://www.noniuss.com>.
- [38] SAINT, Bruker AXS, **2007**; G. M. Sheldrick, *SADABS*, Bruker AXS, **2004–2008**.
- [39] G. M. Sheldrick, H. A. Hauptman, C. M. Weeks, R. Miller, I. Usón, “Ab initio phasing” in *International Tables for Crystallography* (Eds.: M. G. Rossmann, E. Arnold), IUCr and Kluwer Academic Publishers, Dordrecht, **2001**, vol. F, p. 333–351; G. M. Sheldrick, *SHELXD*, University of Göttingen and Bruker Nonius, **2000–2004**.
- [40] P. van der Sluis, A. L. Spek, *Acta Crystallogr., Sect. A* **1990**, *46*, 194.
- [41] A. L. Spek, *PLATON*, Utrecht University, The Netherlands, **2008**; A. L. Spek, *J. Appl. Crystallogr.* **2003**, *36*, 7.
- [42] L. Zsolnai, G. Huttner, *XPMA*, University of Heidelberg, **1994**; <http://www.uni-heidelberg.de/institute/fak12/AC/huttner/software/software.html>.
- [43] R. Soltek, *Winray 32*, University of Heidelberg, **2000**; <http://www.uni-heidelberg.de/institute/fak12/AC/huttner/software/software.html>.
- [44] a) R. Ahlrichs, M. Bär, M. Häser, H. Horn, C. Kölmel, *Chem. Phys. Lett.* **1989**, *162*, 165–169; b) O. Treutler, R. Ahlrichs, *J. Chem. Phys.* **1995**, *102*, 346–356; c) K. Eichkorn, F. Weigend, O. Treutler, R. Ahlrichs, *Theor. Chem. Acc.* **1997**, *97*, 119–124.
- [45] a) A. D. Becke, *Phys. Rev. A* **1988**, *38*, 3098–3100; b) J. P. Perdew, *Phys. Rev. B* **1986**, *33*, 8822–8824.
- [46] F. Weigend, R. Ahlrichs, *Phys. Chem. Chem. Phys.* **2005**, *7*, 3297–3305.

Received: June 26, 2009
Published Online: October 8, 2009